ERDC/GSL TR-15-13

Geotechnical and Structures Laboratory

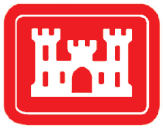

US Army Corps
of Engineers®
Engineer Research and
Development Center

ERDC
INNOVATIVE SOLUTIONS
for a safer, better world

Field Jet Erosion Tests on the Mississippi River Collocated Demonstration Section, Plaquemines Parish, Louisiana

Johannes L. Wibowo, Perry A. Taylor, Bryant A. Robbins,
and Eric W. Smith

June 2015

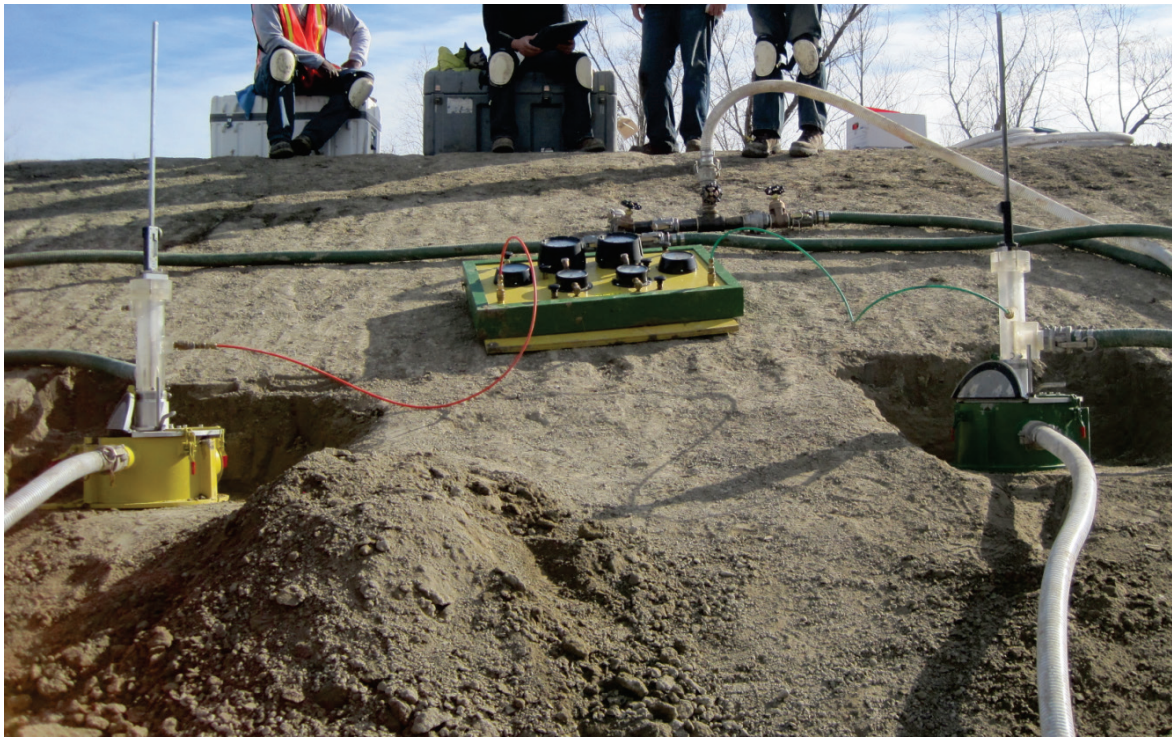

The U.S. Army Engineer Research and Development Center (ERDC) solves the nation's toughest engineering and environmental challenges. ERDC develops innovative solutions in civil and military engineering, geospatial sciences, water resources, and environmental sciences for the Army, the Department of Defense, civilian agencies, and our nation's public good. Find out more at www.erdc.usace.army.mil.

To search for other technical reports published by ERDC, visit the ERDC online library at http://acwc.sdp.sirsi.net/client/default.

ERDC/GSL TR-15-13
June 2015

Field Jet Erosion Tests on the Mississippi River Collocated Demonstration Section, Plaquemines Parish, Louisiana

Johannes L. Wibowo, Perry A. Taylor,
Bryant A. Robbins, and Eric W. Smith

Geotechnical and Structures Laboratory
U.S. Army Engineer Research and Development Center
3909 Halls Ferry Road
Vicksburg, MS 39180-6199

Final report

Prepared for U.S. Army Corps of Engineers
Washington, DC 20314-1000

Abstract

Field jet erosion tests (JETs) were conducted by the U.S. Army Engineer Research and Development Center (ERDC) to assess the erodibility of two enlargement segments within the Mississippi River Levee (MRL) Collocated Demonstration Section in Plaquemines Parish, Louisiana. The first segment was constructed of Bonnet Carré clay with a fly-ash/bed-ash blend treatment, and the second segment was constructed of Bonnet Carré clay treated with lime. In addition, a section of untreated clay on the original levee was also tested. The field JET data showed that the clay treated with lime was categorized as resistant to very resistant. The fly-ash/bed-ash-treated clay was categorized as moderately resistant and resistant. When compared to the existing, untreated clay levee, both treatments reduced the erodibility of the soil. However, the field JET results showed that lime treatment performed better at reducing erosion than the fly-ash/bed-ash treatment.

Contents

Figures and Tables

Figures

Tables

Preface

This study was conducted for the U.S. Army Corps of Engineers, New Orleans District (USACE-MVN). The Technical Monitor was Jehu B. Johnson. This report was published under Infrastructure Technology of the Navigation Structures Program.

The work was performed by the Geotechnical Engineering and Geosciences Branch (GEGB) of the Geosciences and Structures Division (GSD), U.S. Army Engineer Research and Development Center, Geotechnical and Structures Laboratory (ERDC-GSL). At the time of publication, Chad A. Gartrell was Chief, CEERD-GSG; Bartley P. Durst was Chief, CEERD-GS; and Dr. Michael K. Sharp, CEERD-GZT, was the Technical Director for Water Resources Infrastructure. The Acting Deputy Director of ERDC-GSL was Dr. Will McMahon, and the Acting Director was Dr. William P. Grogan.

LTC John T. Tucker III was the Acting Commander of ERDC and Dr. Jeffery P. Holland was the Director.

The U.S. Army Engineer Research and Development Center (ERDC) would like to acknowledge and thank New Orleans District for the funding, field support, and opportunity given to the ERDC team in performing this study.

Unit Conversion Factors

Multiply	By	To Obtain
feet	0.3048	meters
gallons (US liquid)	3.785412 E-03	cubic meters
inches	0.0254	meters
pounds (mass) per cubic foot	16.01846	kilograms per cubic meter

1 Introduction

Field jet erosion tests (JETs) were performed to assess the erodibility of two treated levee enlargements of the Mississippi River Levee (MRL) Collocated Demonstration Section in Plaquemines Parish, LA, and one untreated segment of the original levee. One of the treated segments was constructed of Bonnet Carré high plasticity clay (CH) with a fly-ash/bed-ash blend treatment, and the other segment was constructed of CH with lime treatment. Both treated sections were 350 ft in length. Eight JETs were performed on the segment with fly-ash/bed-ash treatment: two tests at the landside toe, four tests at the landside middle slope, and two tests at the riverside middle slope. Four tests were conducted on the segment with lime treatment: two tests at the toe and two tests mid-slope on the landside of the levee. Four tests were performed on the untreated clay embankment segment as a comparison. In total, the U.S. Army Engineer Research and Development Center (ERDC) performed 16 field JETs. The locations for the tests were discussed with representatives from the U.S. Army Corps of Engineers (USACE), New Orleans District (MVN). After confirmation from MVN of the test locations, the positions were marked in the field using a handheld global positioning system (GPS) device.

The field JET results showed that lime treatment performed better than the fly-ash/bed-ash treatment in reducing erosion. This finding is different when compared to the results of a laboratory erodibility study performed by the Texas Transportation Institute using an erosion function apparatus (EFA) (Oh and Briaud 2010) and also differs from results of laboratory JETs conducted by USACE, Savannah District (SAS) (Wielputz 2010). The results from the tests conducted by Texas Transportation Institute were similar to results recorded by Wielputz (2010).

2 Field Jet Erosion Test

ERDC deployed two JET apparatuses to the MRL Demonstration Section. The apparatuses used were identical to the JET apparatus owned by the National Sedimentation Laboratory (NSL) of the U.S. Department of Agriculture (USDA) in Oxford, MS, as a means to predict the erodibility of cohesive bank materials (Hanson et al. 2002). As described in Hanson (1991), the NSL developed a soil-dependent "jet index" based on the change in maximum scour depth caused by an impinging jet of water versus time. The JET consists of placing the testing device on the soil surface and allowing a submerged water jet to impinge on and scour the soil surface. The scoured hole depth is then measured as a function of time, and analytical procedures are used to measure the soil erodibility parameters. The test method and apparatus are described in ASTM (2007a).

2.1 Testing apparatus

Figure 1 shows the testing apparatus designed by the USDA, Agricultural Research Service, to operate with a constant water pressure from an attached head tank. This apparatus maintains a nonfluctuating pressure head and was designed for testing natural geologic materials of relatively lower density.

The NSL modified the apparatus to include a water pump that provides an alternative water pressure source and eliminates the head tank. The pressure may fluctuate, but this modified apparatus accommodates erosion testing on more dense geologic material. Figure 2 shows the modified JET apparatus used for this project.

2.2 Jet erosion test theory

The general expression of the rate of erosion is found in Hanson (1991) as

$$\varepsilon = k_d\left(\tau_e - \tau_c\right) \tag{1}$$

where:

k_d = the erodibility coefficient (cm³/N-s)
τ_e = the effective stress (Pa)
τ_c = the critical stress (Pa)

Figure 1. Original JET apparatus using constant water head system (Hanson and Cook 2004, reprinted with permission).

Figure 2. NSL-modified JET apparatus using an alternate water pressure source.

Equation 1 describes the physical phenomena of erosion and states that the rate of erosion is proportional to the difference between effective stress and critical stress, as well as the erodibility coefficient.

Hanson (1991) initiated the development of an erosion testing apparatus as shown schematically in Figure 3 for various geologic materials based on the change of erosion depth as a function of jet pressure and time. The details of the procedure are described in ASTM (2007a). As an enhancement to the procedure, Hanson and Cook (1999) removed the empirical factor and directly measured the excessive stress based on the diffusion principle of a submerged circular jet and scour under jet impingement as proposed by Stein and Nett (1997). The initial stress of circular flow, τ_i, is then expressed as

$$\tau_i = \tau_0 \left(\frac{J_p}{J_i} \right)^2 \tag{2}$$

$$J_p = C_d d_0 \tag{3}$$

$$\tau_0 = C_f \, \rho \, U_0^2 \tag{4}$$

$$U_0 = \sqrt{2gh} \tag{5}$$

where:

τ_i = initial peak boundary stress before scour
τ_o = the maximum stress within potential core
J_p = the potential core length
J_i = the initial height
J_e = the erosion equilibrium depth
C_d = diffusion constant = 6.3
d_o = nozzle diameter
C_f = friction coefficient
ρ = fluid density
U_o = velocity at the jet nozzle
g = gravity
h = differential head

Figure 3. Schematic diagram of the jet erosion process (Hanson and Cook 2004, reprinted with permission).

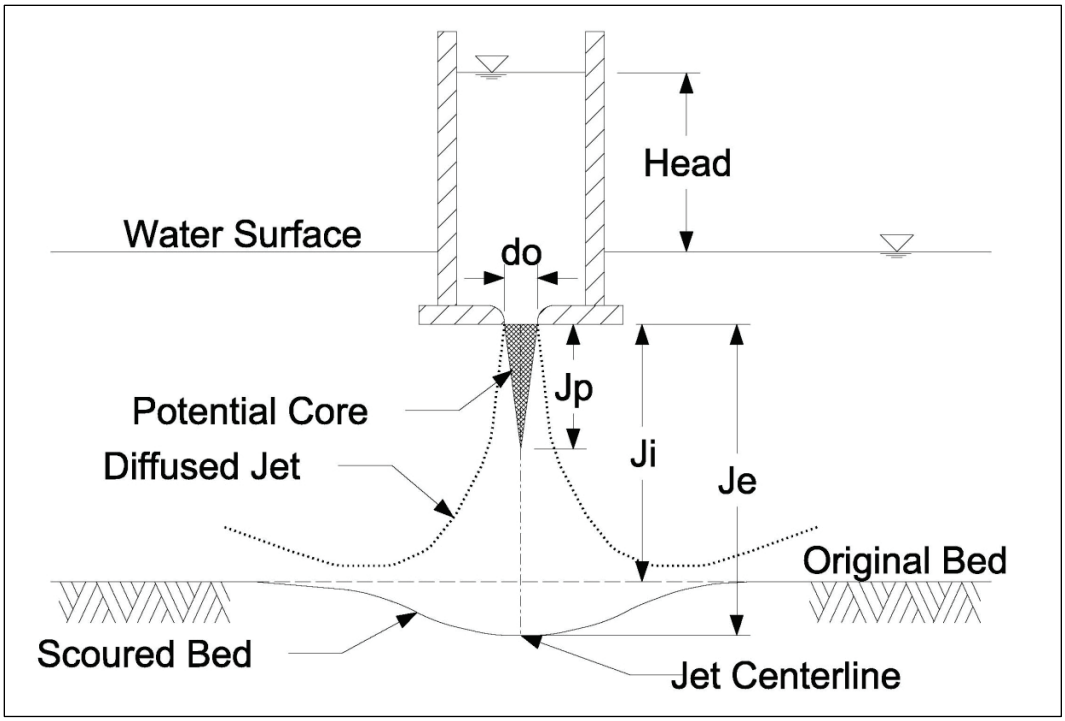

To calculate the equilibrium scour depth, Hanson and Cook used the expression proposed by Blaisdell et al. (1981) that assumed the scour rate conforms to a logarithmic hyperbolic function. The excess stress parameter, τ_c, is predetermined by fitting the observed scour data to this logarithmic hyperbolic curve. The erodibility coefficient, k_d, is then determined by curve fitting the actual measurement of scour depth, H, versus time, t. A detailed discussion on determining the erodibility coefficient can be found in Hanson and Cook (1999, 2004).

3 Test Segments

The demonstration levee is located in Plaquemines Parish, LA, at Belle Chasse, south of New Orleans, parallel to Main Street at the intersection with F. Edward Hebert Boulevard as shown in Figure 4. The test section consisted of two segments: clay levee with fly-ash treatment and clay levee with lime treatment (Figure 4). An untreated section of the original clay levee was also tested. Tests 1, 2, 3, and 4 were performed on the untreated clay levee. Test 5, 6, 7, 8, 13, 14, 15, and 16 were done on the clay levee treated with fly ash. Tests 9, 10, 11, and 12 were performed on the clay levee treated with lime. The coordinates of each test were obtained using a handheld GPS (Table 1).

Figure 4. Location of JETs on the Collocated Demonstration Section, Plaquemines Parish, LA.

Table 1. The coordinates of each test location.

Test No.	Latitude	Longitude
1 & 2	N 29.88484°	W 089.97034°
3 & 4	N 29.88482°	W 089.97024°
5 & 6	N 29.88454°	W 089.97096°
7 & 8	N 29.88455°	W 089.97100°
9 & 10	N 29.88423°	W 089.97215°
11 & 12	N 29.88417°	W 089.97225°
13 & 14	N 29.88445°	W 089.97115°
15 & 16	N 29.88450°	W 089.97117°

4 Field Testing Procedure

The following is a summary of the field test procedure:

1. After selecting the testing site, the equipment was mobilized to the site. Because the testing apparatuses required a constant water supply and the water source was about 400 ft away, a 500-gal reservoir tank was used at the site. A water truck provided by MVN continuously supplied water to the tank. For each test location, four to six tests were performed to consider the possibility of material variability in the chosen location.
2. Two sites were prepared about 6 ft apart for the two JET apparatuses by removing grass, roots, or any gravelly material. Prior to clearing the sites, photographs were taken of the original surface. A density test was performed on similarly prepared surfaces adjacent to test sites so as not to influence the JET data. Disturbed soil samples were taken for water content measurement, grain-size analysis, and Atterberg limit tests. The JET apparatuses were then placed over the prepared surface.
3. The steel testing chamber was driven about 1 in. into the soil surface using a special driving hammer. The Plexiglas cover (composed of a Plexiglas tube frame, jet nozzle unit, point gauge unit, and pressure gauge) was placed on top of the tank, and the inlet water supply hose was connected.
4. The point gauge initial reading was used to determine the distance from the jet mouth to the ground surface. The jet testing chamber was then filled with water by opening the inlet valve with the deflector in front of the jet nozzle to prevent premature surface erosion. The water pressure was adjusted to a target pressure.
5. Scour depth readings were noted on a data sheet (Figure 5). A recording time interval was set, depending on the surface soil material. The more erodible material required a smaller time step interval than less erodible soils.
6. The test began by removing the deflector from the front of the jet nozzle and starting the stopwatch. The water from the jet nozzle eroded the ground surface and, at the chosen time interval, the test was stopped by positioning the deflector underneath the center of the jet and lowering the point gauge rod to close the jet nozzle. The point gauge rod was then lowered to the eroded surface to measure the amount of erosion. After manually recording the data, the rod was positioned above the deflector

plate, the deflector was again placed in front of the jet nozzle, the point gauge was raised (thereby opening the jet nozzle), and the next time-step test was begun.

Figure 5. Example data sheet for one apparatus at one test location.

STREAM BED JET DATA

DATE 1/26/2011

JET TEST LOCATION Plaquemines Levee with fly ash

OPERATOR ERDC

ZERO POINT GAGE READING 1.370

TEST # 5

PRELIMINARY HEAD SETTING 15

PT GAGE RDG @ NOZZLE 1.621

NOZZLE DIAMETER (IN) 0.25

NOZZLE HEIGHT (FT) 0.251

SCOUR DEPTH READINGS

TIME (MIN)	DIFF TIME (MIN)	PT GAGE READING (FT)	MAXIMUM DEPTH OF SCOUR (FT)
0	0	1.370	0.000
2	2	1.364	0.006
4	2	1.354	0.016
9	5	1.343	0.027
19	10	1.330	0.040
21	2	1.321	0.049
26	5	1.297	0.073
31	5	1.266	0.104
36	5	1.232	0.138
41	5	1.210	0.160
46	5	1.198	0.172
56	10	1.182	0.188

HEAD SETTING

TIME (MIN)	HEAD (IN)
0	415.65
2	415.65
4	554.20
9	554.20
19	562.51
21	831.30
26	831.30
31	831.30
36	831.30
41	831.30
46	831.30
56	831.30

7. After recording the depth/time readings from each of the two apparatuses, the water pressure was readjusted to the original value and the above procedures were repeated to obtain about 10 to 12 additional data points. Figure 6 shows the cumulative erosion versus time.

Figure 6. Example of erosion as a function of time.

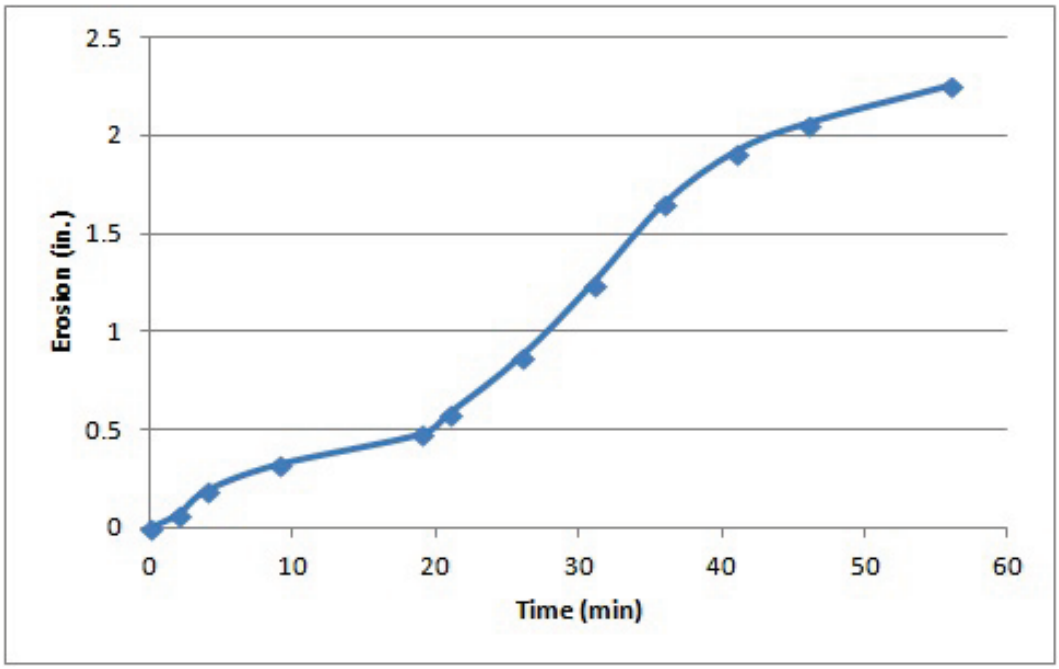

5 Tests and Results

5.1 Untreated clay segment

The untreated clay segment, constructed of dark brown, high plasticity clay, was well compacted with a wet density ranging between 110 and 116 pcf. The water content during the test ranged from 26 percent to 41 percent. The levee was well covered with grass. Figure 7 shows a photograph of the ERDC team performing a JET on the untreated clay section. Figure 8 shows the photographs of Test 1 before and after a JET was performed. Figure 9 depicts the progress of erosion depth of Test 1 as a function of time.

Figure 7. The ERDC team performing an erosion field JET on the untreated clay segment.

Figure 8. Test 1, untreated clay segment, (a) before and (b) after a field JET was performed.

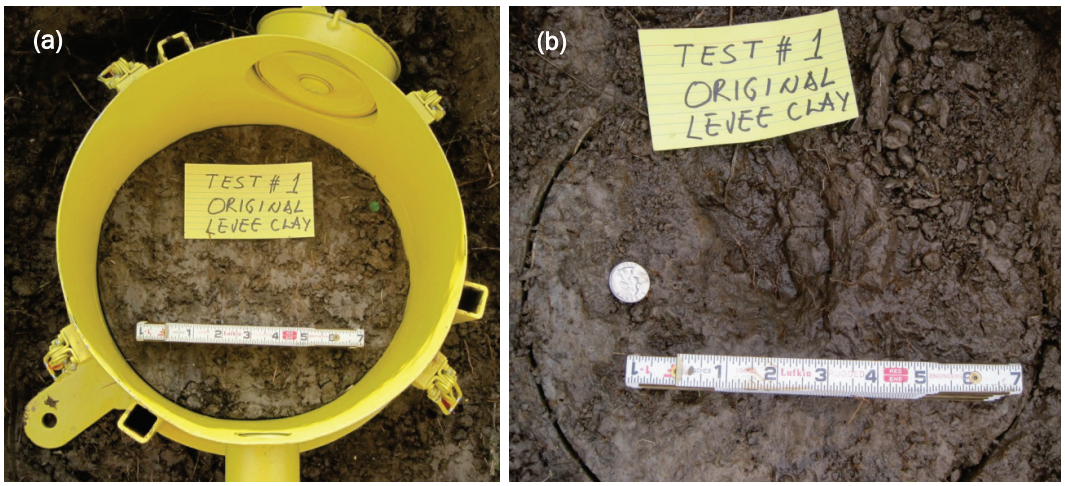

Figure 9. Cumulative erosion depth (in.) versus time (min) of Test 1, on the untreated clay segment.

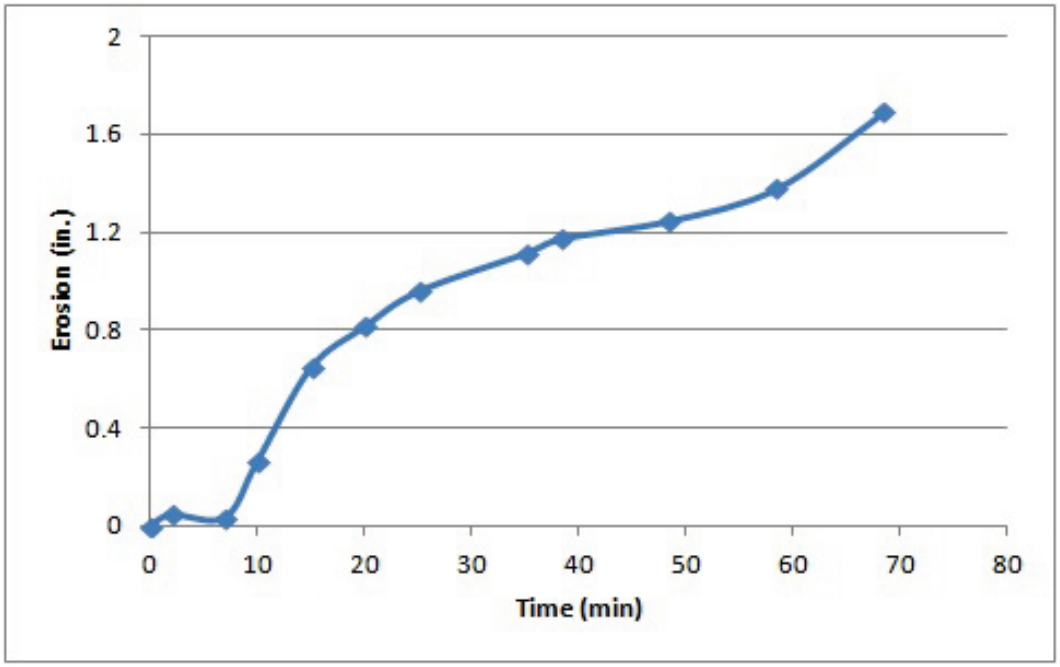

The erodibility coefficient, k_d, and critical shear stress, τ_c, were calculated using a Microsoft Excel spreadsheet and the Solver utility (Figure 10). The solution procedure begins by fitting the recorded scour depths and time of measurement to an asymptotic function that predicts the equilibrium scour depth at $t = \infty$. The corresponding stress that produces the depth of equilibrium scour is defined as the critical shear stress. A summary of k_d and corresponding τ_c for the original clay levee material is shown in Table 2. Additional photographs and the graphs of test results for the untreated clay section are in Appendix A.

Table 2. Summary of field JETs on the untreated clay segment.

Test No.	Location	k_d cm³/N-s	τ_c Pa	Category
1	Clay Levee, Landside	0.156	5.762	Moderately Resistant
2	Clay Levee, Landside	0.141	7.796	Moderately Resistant
3	Clay Levee, Landside	0.112	65.536	Resistant
4	Clay Levee, Landside	0.234	19.503	Moderately Resistant

Figure 10. Plot of erodibility coefficient and critical shear stress of the untreated clay segment using erodibility categories proposed by Hanson and Simon (2001).

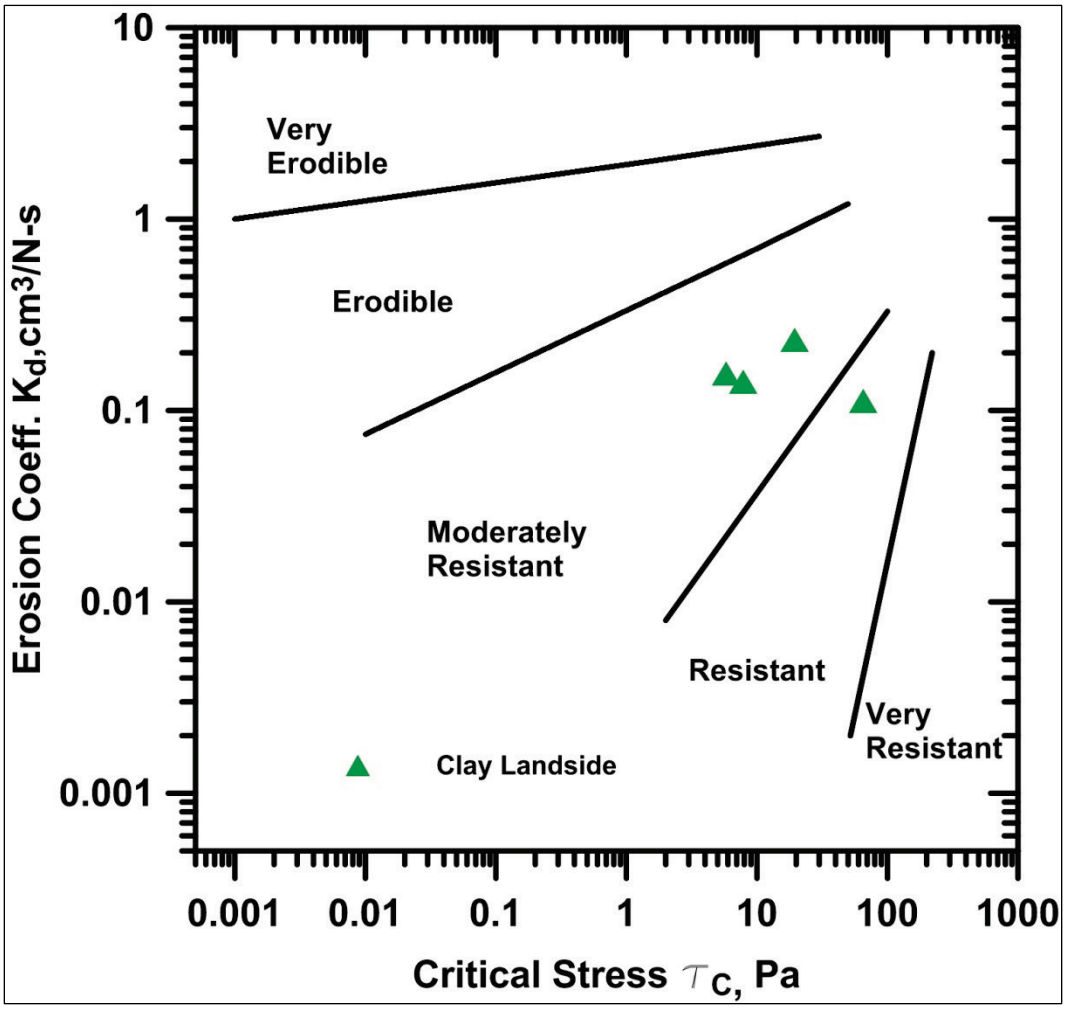

5.2 Clay segment with fly-ash/bed-ash treatment

The additional levee cover is made of a mixture of Bonnet Carré clay with 10 percent of fly-ash/bed-ash. This treatment is intended to create levee material that is strong in resisting overtopping erosion. Laboratory erosion tests using an EFA indicated that this mixture has a high resistance against overtopping erosion (Oh and Briaud 2010). Oh and Briaud (2010) mixed

Bonnet Carré clay with fly-ash and bed-ash and compacted the mixture immediately to the target density of 92 percent using the Standard Proctor Compaction Test. The EFA test result of this mixture is categorized as very low erodibility. USACE, SAS, performed a JET on fly-ash/bed-ash-treated specimen following ASTM (2007a), and the test result showed that the erodibility of the specimen was classified as high resistant (Wielputz 2010).

Figure 11 shows a typical cross section of the demonstration levee, which was raised about 5 ft with a crest width of 11 ft using fly-ash/bed-ash-treated clay or lime-treated clay. The additional compacted-fill part had a steeper slope (1V:2H) than the original slope (1V:3H).

Figure 11. Typical cross section of the levee demonstration site. The enlargement was constructed of clay treated with fly-ash/bed-ash, or lime (USACE 2010).

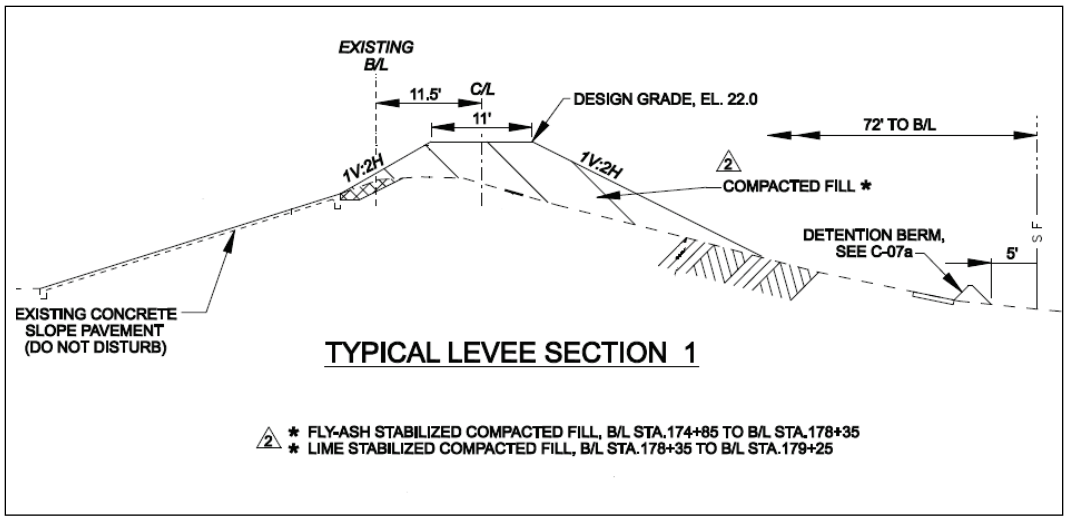

The Bonnet Carré clay was mixed with fly-ash/bed-ash and stockpiled for four to six weeks before the contractor started construction (Johnson 2011). The soil was compacted by two passes of a padsfoot roller. The JETs were performed on the treated levee approximately three months after construction. Six field JETs were performed on the landside of the levee, and two tests were done on the riverside of the levee enlargement. The treated levee material was grayish black plastic clay with wet density ranging from 105 to 110 pcf. The water contents ranged between 31 percent and 38 percent at the test locations. Figure 12 shows a photograph of the engineers from the ERDC team performing a JET on the fly-ash/bed-ash-treated levee. Figure 13 shows photographs of the section treated with fly-ash/bed-ash before and after a JET was performed. Figure 14 depicts the progress of erosion depth as a function of time. The value of k_d and τ_c are

tabulated in Table 3, and the data are plotted on the erosion category chart proposed by Hanson and Simon (2001) as shown in Figure 15. Additional photographs and graphs of test results for the clay levee with fly-ash/bed-ash treatment can be found in Appendix B.

Figure 12. Engineers from ERDC performing field JET on fly-ash/bed-ash-treated segment.

Figure 13. Test 5, clay segment with fly-ash/bed-ash treatment, (a) before and (b) after a field JET was performed.

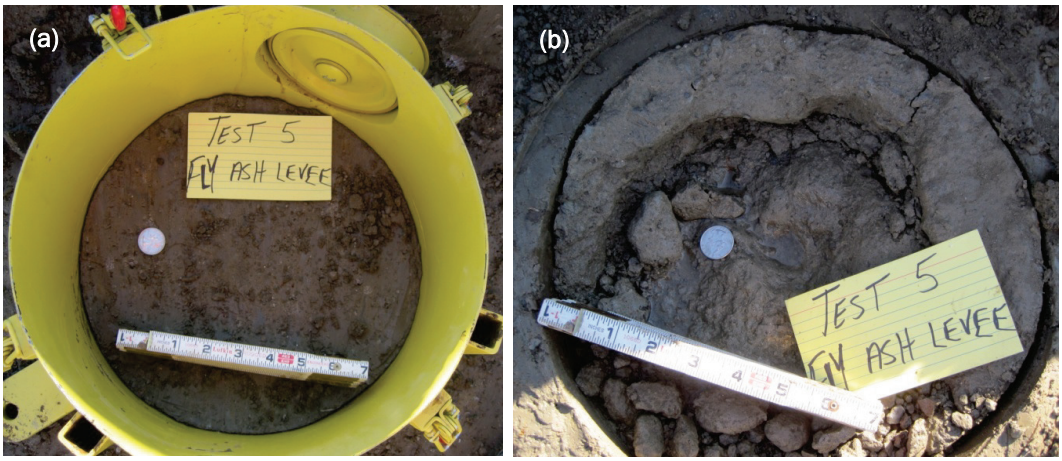

Figure 14. Cumulative erosion depth (in.) versus time (minutes) of Test 5, clay segment with fly-ash/bed-ash treatment.

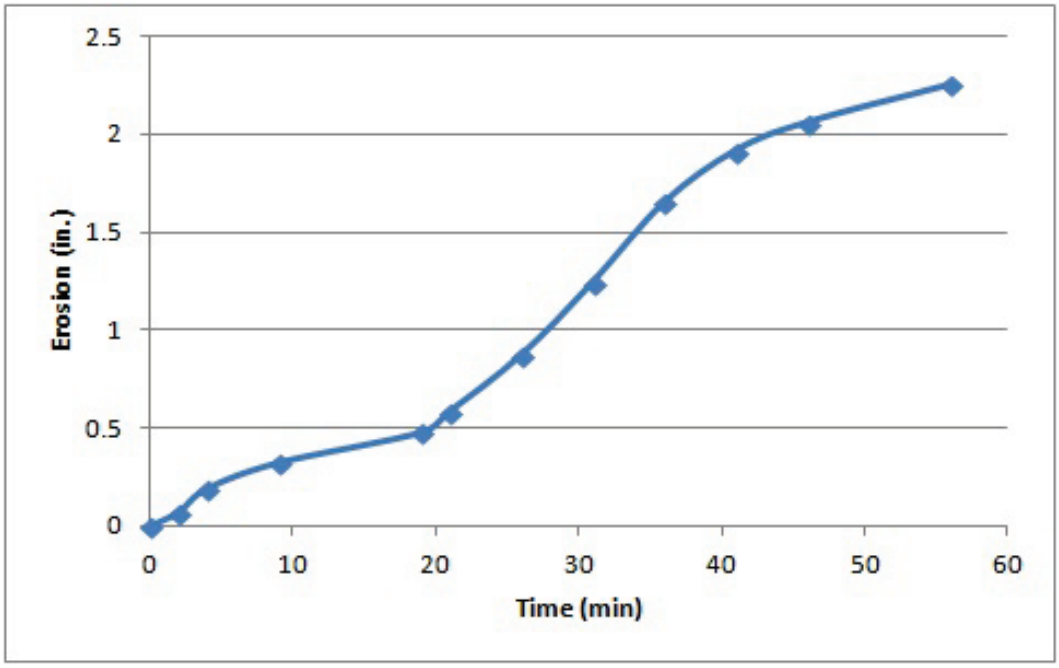

Table 3. Summary of field JETs on clay segment with fly-ash and bed-ash treatment.

Test No.	Location	k_d cm³/N-s	τ_c Pa	Category
5	Clay with Fly ash, Landside	0.088	2.899	Moderately Resistant
6	Clay with Fly ash, Landside	0.056	16.371	Resistant
7	Clay with Fly ash, Landside	0.225	18.229	Moderately Resistant
8	Clay with Fly ash, Landside	0.191	30.225	Moderately Resistant
13	Clay with Fly ash, Riverside	1.875	0.841	Erodible
14	Clay with Fly ash, Riverside	0.520	12.272	Moderately Resistant
15	Clay with Fly ash, Landside	0.133	8.899	Moderately Resistant
16	Clay with Fly ash, Landside	0.192	3.408	Moderately Resistant

Figure 15. Plot of erodibility coefficient and critical shear stress of fly-ash/bed-ash-treated clay using the erodibility category proposed by Hanson and Simon (2001).

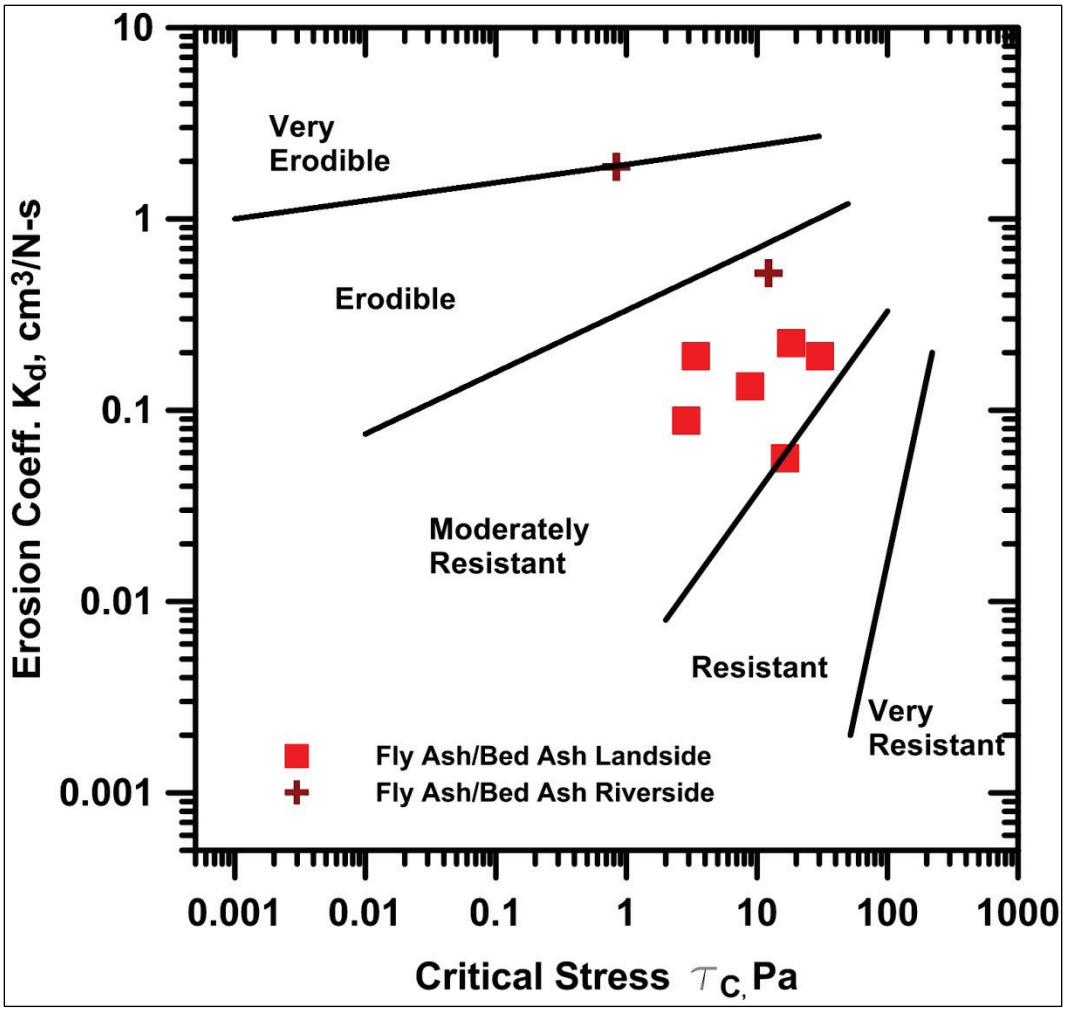

5.3 Clay segment with lime treatment

The levee enlargement in this test section was constructed of Bonnet Carré clay treated with 8 percent lime by dry weight. The purpose of this treatment was to increase the resistance of the levee surface to overtopping erosion. Laboratory erosion tests using an EFA indicated that this mixture has a high erosion resistance (Oh and Briaud 2010). Oh and Briaud (2010) mixed Bonnet Carré clay with three different percentages of lime, 6 percent, 4 percent, and 5 percent, and compacted the mixture immediately following mixing to a target density of 92 percent of maximum dry density of Standard Proctor Compaction Test (ASTM 2007b). The EFA test result of this mixture is categorized as very low erodibility. The USACE, SAS, (Wielputz 2010) performed a JET on a lime-treated specimen following

ASTM D 5852 (ASTM 2007a), and the test result showed that the erodibility of the specimen is classified as high resistance.

The typical cross section of the lime-treated levee enlargement is similar to the fly-ash/bed-ash-treated segment (Figure 10), except that it has a crest width of 18 ft. The levee was raised about 5 ft using the treated mixtures. The additional compacted fill part has a steeper slope (1V:2.5H) as compared to the original slope (1V:3H).

Similar to the fly-ash/bed-ash treatment, the Bonnet Carré clay was mixed with 8 percent lime and stockpiled for two to three weeks before construction. The construction of this mixture was different than the fly-ash/bed-ash mixture. To reach the density close to 92 percent maximum dry density of Standard Proctor Density, the mixture required six passes of a sheepsfoot roller. The treated levee material was grayish light brown CH with density ranging between 99 and 106 pcf. The water contents ranged between 32 percent and 36 percent at the different test locations.

Figure 16 is a photograph of the ERDC team performing a JET on the lime-treated levee. Figure 17 shows photographs of the lime-treated clay levee before and after JETs were performed. Figure 18 depicts the progress of erosion depth as a function of time. The values for k_d and τ_c are tabulated in Table 4, and the data are plotted on the erosion category chart proposed by Hanson and Simon (2001) as shown in Figure 19. Additional photographs and graphs of test results for the clay section with lime treatment are in Appendix C.

Figure 16. The ERDC team performing a field JET test on the lime-treated segment of the levee.

Figure 17. Test 11, clay segment of the levee with lime treatment, (a) before and (b) after a field JET was performed.

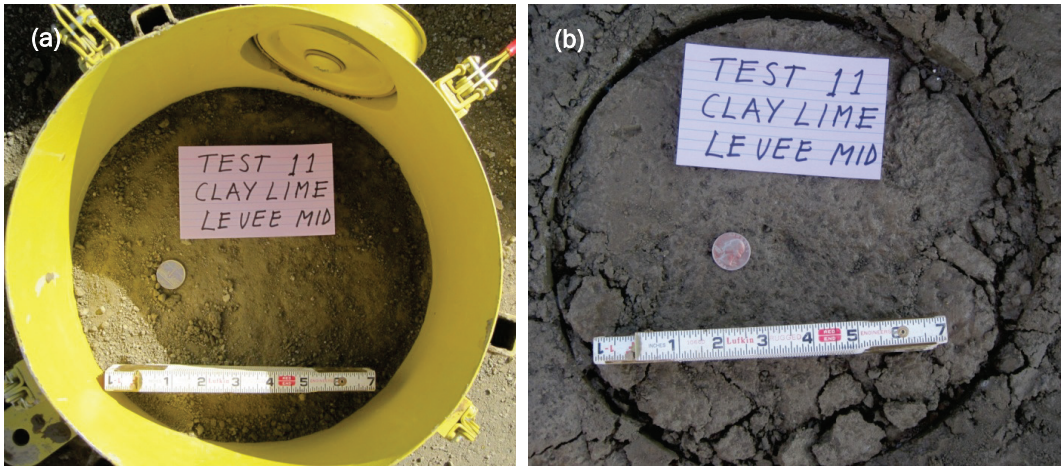

Figure 18. Cumulative erosion depth (in.) versus time (min) of Test 11, section of the clay segment with lime treatment.

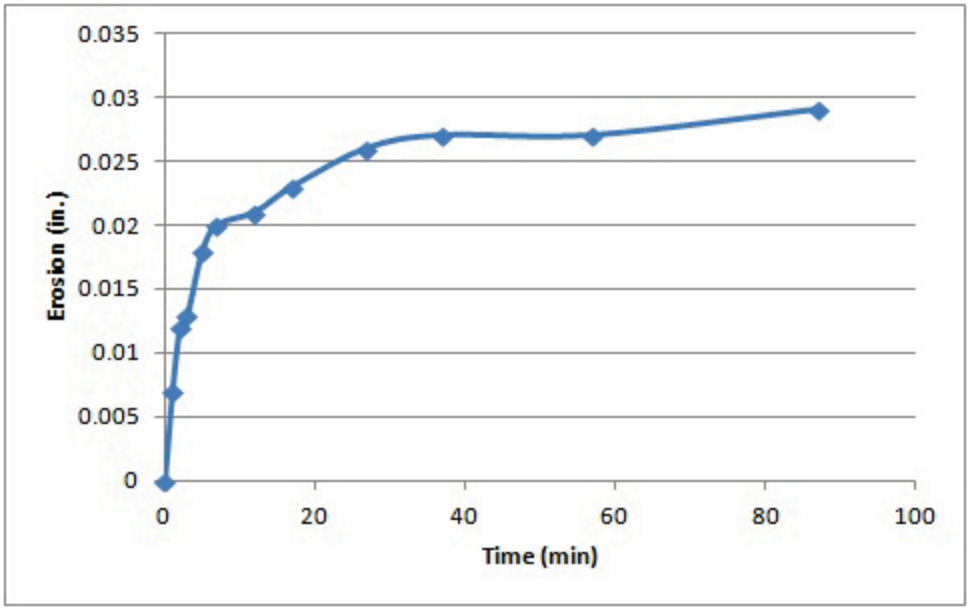

Table 4. Summary of field JETs on the clay segment with lime treatment.

Test No.	Location	k_d cm³/N-s	τ_c Pa	Category
9	Clay with Lime, Landside	0.167	22.247	Moderately Resistant
10	Clay with Lime, Landside	0.260	8.592	Questionable Data
11	Clay with Lime, Landside	0.024	157.251	Very Resistant
12	Clay with Lime, Landside	0.094	120.201	Very Resistant

Figure 19. Plot of erodibility coefficient and critical shear stress of lime treatment using the erodibility categories proposed by Hanson and Simon (2001).

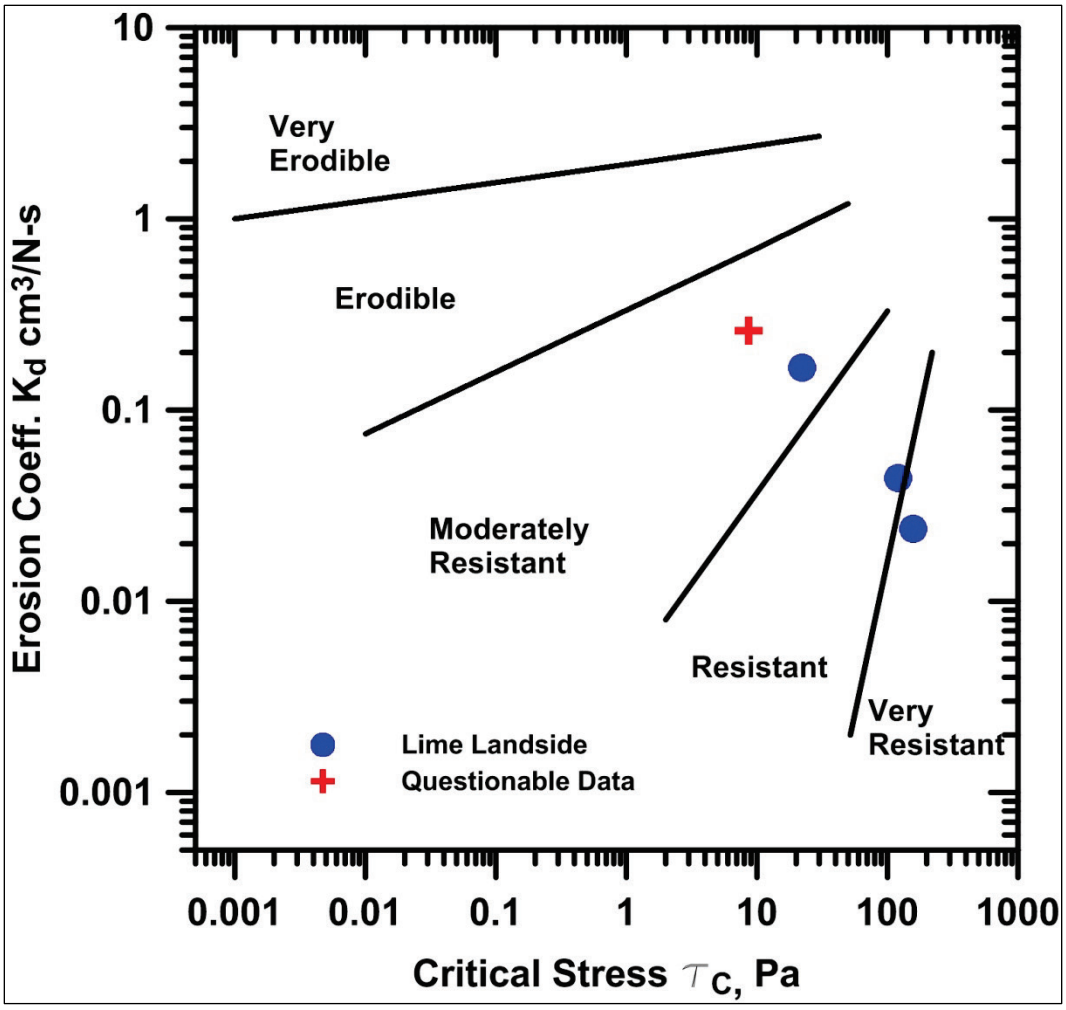

6 Discussion

In an ideal situation, the erosion progress versus time curve would show an asymptotic type of curvature, which indicates that erosion had approached an equilibrium stage. However, several plots using results from JETs conducted for this study showed a sudden increase in erosion after achieving a small amount of steady erosion at an established rate. This phenomenon indicated that the compacted fill is not homogeneous. The lack of homogeneity is caused by the procedure used in levee construction. This nonhomogeneous behavior was especially seen on the riverside of the embankment. It is believed that this behavior is due to the embankment shape inhibiting proper mechanical compaction of the material near the riverside edge of the enlargement. Because of these issues, one JET may capture two different blocks of compacted soil mixtures. Depending on the individual data recorded, additional values (secondary data) of erodibility coefficient, k_d, and critical stress, τ_c, can be calculated. Figure 20 shows an example of this phenomenon from Test 15 on the levee segment with fly-ash/bed-ash treatment. The bottom curve recorded a 0.1-in. erosion increment and suddenly about 1 in. of erosion occurred. After the sudden increase, the levee materials experienced a small increment of erosion. The rapid increase followed by a lower rate of erosion indicated that the tested levee materials consisted of two different materials, or, in other words, the levee is nonhomogeneous. The erodibility parameters of the near surface part are given by k_d equal to 0.561 cm^3/N-s and a τ_c equal to 48.555 Pa, which is categorized as moderately resistant; whereas, the erodibility of the deeper layers is given by k_d equal to 0.049 cm^3/N-s and a τ_c equal to 52.480 Pa, which is categorized as resistant. The combining of primary data and secondary data yields a k_d equal to 0.133 cm^3/N-s and a τ_c equal to 8.899 Pa. Each set of recorded data was evaluated this way to identify variance in erodibility between the nonhomogenous portions of the treated levee.

Table 5 shows the summary of k_d and τ_c from primary data and secondary data. The primary data were calculated using all data by assuming that the compacted fill was homogeneous, while the secondary data were calculated using only partial data. There may be more than one set of secondary data per test or no secondary data depending on the original data collected (i.e., the existence of secondary data is dependent on discontinuities in the primary data).

Figure 20. Test 15, segment with fly-ash/bed-ash-treated enlargement, shows the nonhomogeneity of the clay layers.

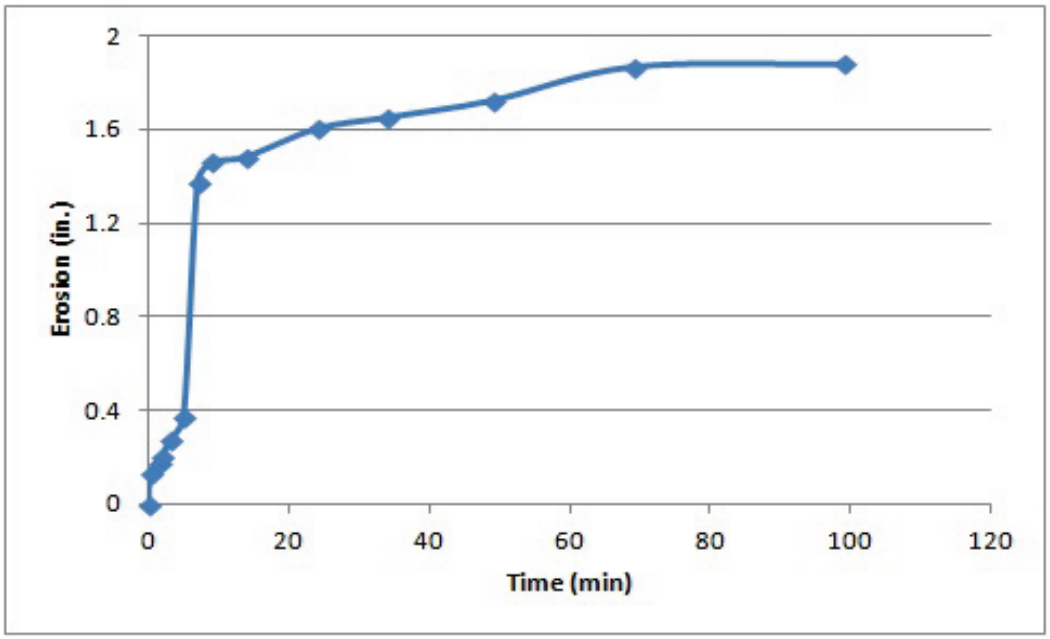

Table 5. Summary of erodibility coefficient, k_d, and critical stress, τ_c, from both primary data and secondary data.

Test No.	Location	Primary			Secondary		
		k_d cm³/N-s	τ_c Pa	Category	k_d cm³/N-s	τ_c Pa	Category
1	Clay Levee, LS	0.156	5.762	MR			
2	Clay Levee, LS	0.141	7.796	MR			
3	Clay Levee, LS	0.112	65.536	R			
4	Clay Levee, LS	0.234	19.503	MR			
5	Clay w/Fly ash, LS	0.088	2.899	MR			
6	Clay w/Fly ash, LS	0.056	16.371	R	0.054	50.433	R
7	Clay w/Fly ash, LS	0.225	18.229	MR	0.167	25.46	MR-R
8	Clay w/Fly ash, LS	0.191	30.225	MR	0.144	39.878	R
9	Clay w/Lime, LS	0.167	22.247	MR			
10	Clay w/Lime, LS	0.260	8.592	MR	0.212	1.659	MR
11	Clay w/Lime, LS	0.024	157.251	VR			
12	Clay w/Lime, LS	0.094	120.201	VR			
13	Clay w/Fly ash, RS	1.875	0.841	E			
14	Clay w/Fly ash, RS	0.52	12.272	MR	0.21	53.483	R
15	Clay w/Fly ash, LS	0.133	8.899	MR	0.561 0.049	48.555 52.480	MR R
16	Clay w/Fly ash, LS	0.192	3.048	MR	0.094	14.797	MR

Note: MR = moderately resistant, R = resistant, VR = very resistant, and E = erodible.

LS = Landside, RS = Riverside

Figure 21 shows the summary of primary test data using the erosion categories proposed by Hanson and Simon (2001). When the primary data and secondary data were combined as shown in Figure 22, the erodibility category of fly-ash/bed-ash-treated clay improved.

One possible explanation for the nonhomogeneous conditions encountered in the field is found in the sequencing implemented in constructing the test sections. USACE and MVN representatives indicated that the fly-ash/bed-ash was mixed with the clay in a stockpile and brought to optimum moisture. After a period of four to six weeks, the soil mixture was remixed, placed, and compacted (Johnson 2011). The delay between fly-ash/bed-ash incorporation and compaction allowed the cementitious compounds to form in the stockpile, thereby agglomerating the soil particles. Remixing the soil breaks these cementitious bonds, which do not reform, thereby reducing the overall strength of the constructed embankment. Fly-ash/bed-ash soil stabilization increases the strength of soil through three mechanisms: cementitious reactions, pozzolanic reactions, and ion exchange. For Class C fly-ash as well as bed-ash in general, the most significant strength gains are achieved by the cementitious reactions. Class C fly-ash is produced from the burning of lignite and subbituminous coal and may also be produced from anthracite or bituminous coal. This class typically has total calcium contents, expressed as calcium oxide (CaO) that are higher than Class F fly ashes (ASTM 2008). Recent studies showed that curing periods of longer than seven days produced only marginal increases in unconfined compressive strength with respect to the gains observed in the first week of curing (Acosta et al. 2003; Misra et al. 2005). Due to these properties of Class C fly-ash, construction specifications commonly require that mixing, compaction, and final shaping be completed in one or two hours of initial mixing (Mackiewicz and Ferguson 2005). By minimizing delay between fly-ash incorporation and compaction, higher strengths and densities will be achieved with minimal compaction effort. In addition to higher strengths, allowing the cementitious bonds to form properly without disturbance will increase the erosion resistance of the fly-ash/bed-ash-treated clay.

Figure 21. Summary of erodibility coefficient and the corresponding critical stress of all primary test data.

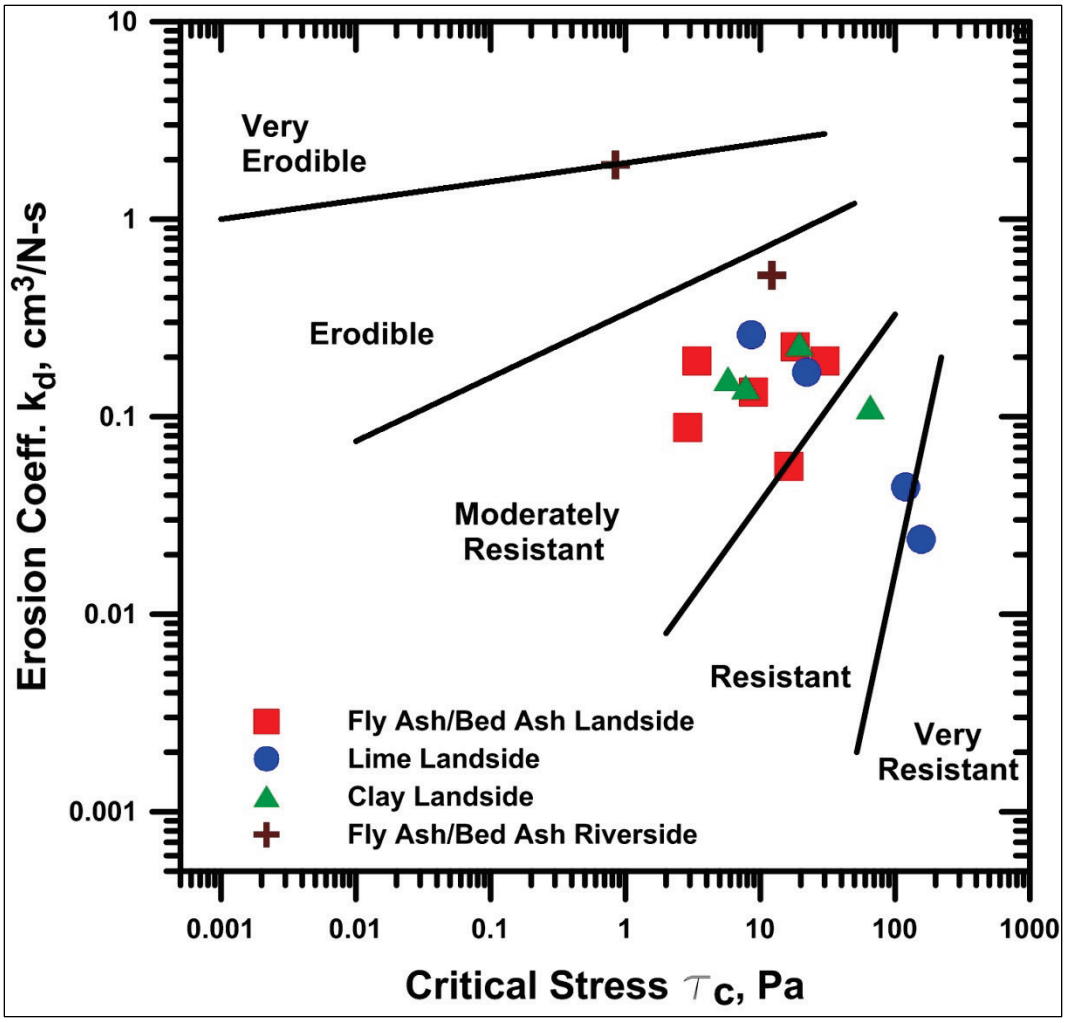

Figure 22. Summary of erodibility coefficient and the corresponding critical stress of all primary and secondary test data.

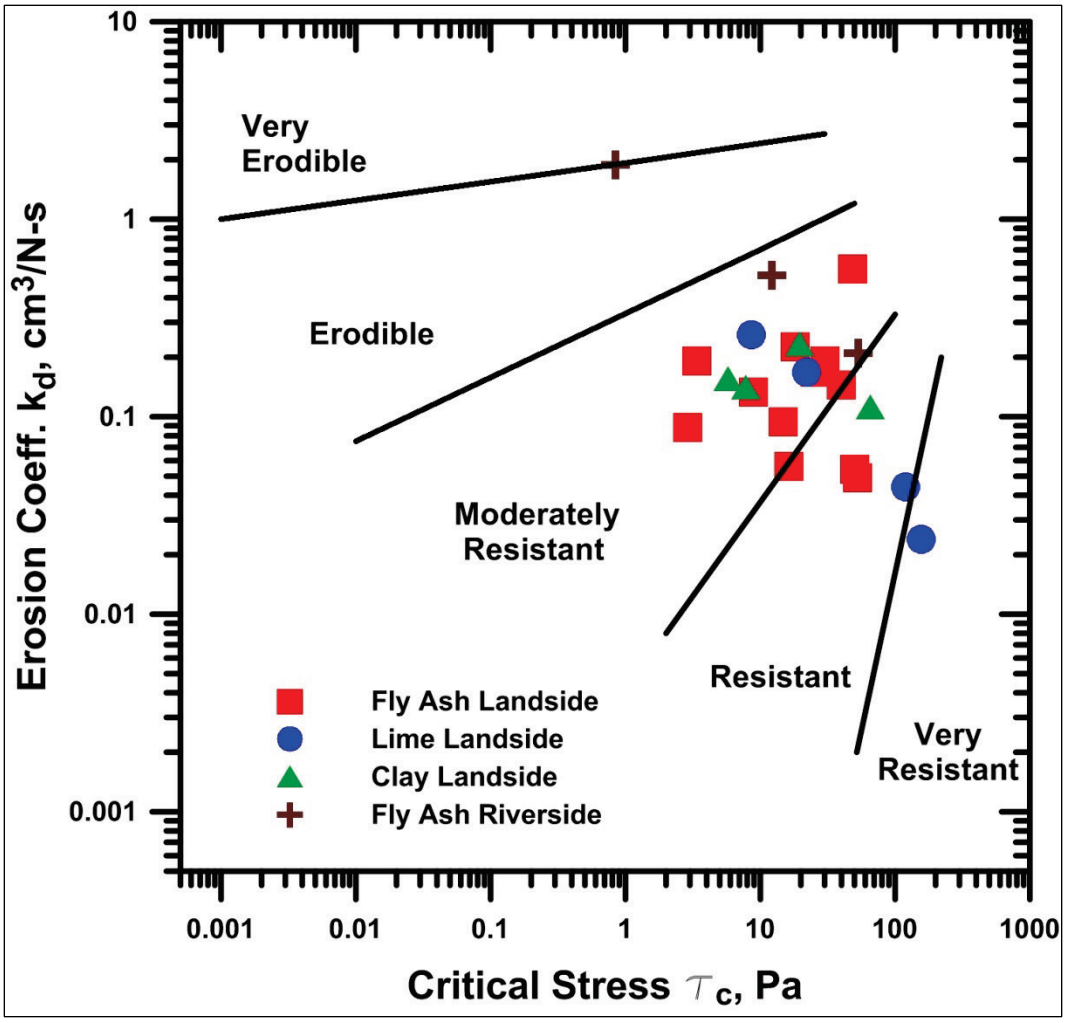

7 Summary and Recommendations

Overall, the field JET data showed that the lime-treated clay can be categorized as resistant to very resistant. The fly-ash/bed-ash-treated clay can be categorized as moderately resistant and resistant. Compared to the untreated clay segment, both treatments reduced the erodibility of the soil. The treated levee enlargements did not have homogeneous compaction as revealed by the discontinuous test results. This nonhomogenous behavior is especially apparent on the fly-ash/bed-ash-treated levee enlargement. The delay between incorporation of fly-ash/bed-ash into the clay and time of compaction will affect the engineering properties of the treated clay material and is one possible explanation for the nonhomogenous behavior exhibited. Quality control, especially regarding treatment mixing and placement procedures, should be adjusted on future treated levee segments to ensure well-compacted, homogenous results. It is recommended that a prescriptive construction specification be developed or adapted to control mixing and placement sequencing when implementing fly-ash treatment.

References

Acosta, H. A., T. B. Edil, and C. H. Benson. 2003. *Soil stabilization and drying using fly ash*. Geo Engineering Report No. 03-03. University of Wisconsin-Madison: Department of Civil and Environmental Engineering.

American Society for Testing and Materials. 2008. *Standard specification for coal fly ash and raw or calcined natural pozzolan for use in concrete*. ASTM Standard Designation C618-12a. West Conshohocken, PA: ASTM.

American Society for Testing and Materials. 2007a. *Standard test method for erodibility determination of soil in the field or in the laboratory by the Jet Index method*. ASTM Standard Designation D 5852-07. West Conshohocken, PA: ASTM.

American Society for Testing and Materials. 2007b. *Standard test method for Laboratory Compaction Characteristics of Soil Using Standard Effort*. ASTM Standard Designation D 698-07. West Conshohocken, PA: ASTM.

Blaisdell, F. W., L. A. Clayton, and G. G. Hebaus. 1981. Ultimate dimension of local scour. *J. Hydraulics Division, ASCE* 107(HY3):327–337.

Hanson, G. J. 1991. Development of a jet index to characterize erosion resistance of soils in earthen spillways. *Transactions of the American Society of Agricultural Engineers* 36(5):2015-2020.

Hanson, G. J., and K. R. Cook. 1999. *Procedure to estimate soil erodibility for water management purposes*. American Society of Agricultural Engineers Paper No. 992133. Proc. Mini–Conf. Advance in Water Quality Modeling. St. Joseph, MI: ASAE.

Hanson, G. J., and K. R. Cook. 2004. Apparatus, test procedures and analytical methods to measure soil erodibility in situ. *Applied Engineering in Agriculture* 20(4):455-462.

Hanson, G. J. and A. Simon. 2001. Erodibility of cohesive streambeds in the loess area of the midwestern USA. *Hydrological Processes* 15:23-38.

Hanson, G. J., A. Simon, and K. R. Cook. 2002. *Non-vertical jet testing of cohesive streambank materials*. American Society of Agricultural Engineers Meeting Paper No. 022119. St. Joseph, MI: ASAE.

Johnson, J. 2011. Personal communication, USACE, New Orleans District engineer.

Mackiewicz, S. M., and E. G. Ferguson. 2005. Stabilization of soil with self-cementing coal ashes. http://www.flyash.info/2005/108mac.pdf.

Misra, A., D. Biswas, and S. Upadhyaya. 2005. Physico-mechanical behavior of self cementing class C fly ash-clay mixtures. *Fuel* 84(11):1410-1422.

Oh, S. J., and J-L. Briaud. 2010. *Erosion function apparatus testing of clay material considered for levee construction in New Orleans*. College Station, TX: Texas Transportation Institute.

Stein, O. R., and D. D. Nett. 1997. Impinging jet calibration of excess shear sediment detachment parameters. *Trans. ASAE* 40(6):1573-1580.

U.S. Army Corps of Engineers. 2010. Engineered advance measure English turn bend WBV-MRL 5.1 – Demonstration Section B/L Sta. 174+00 to B/L Sta. 188+25, Plaquemines Parish, Louisiana. New Orleans District: USACE.

Wielputz, M. 2010. Personal communication, USACE, Savannah District engineer.

Appendix A: Untreated Clay Segment

Figure A1. Test 1, (a) before and (b) after field JET was performed.

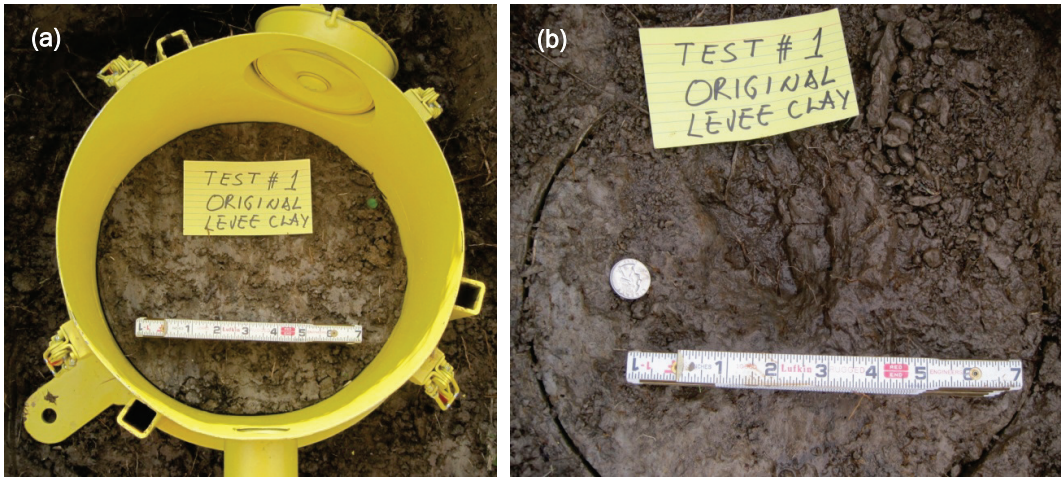

Figure A2. Test 1, cumulative erosion depth (in.) versus time (min).

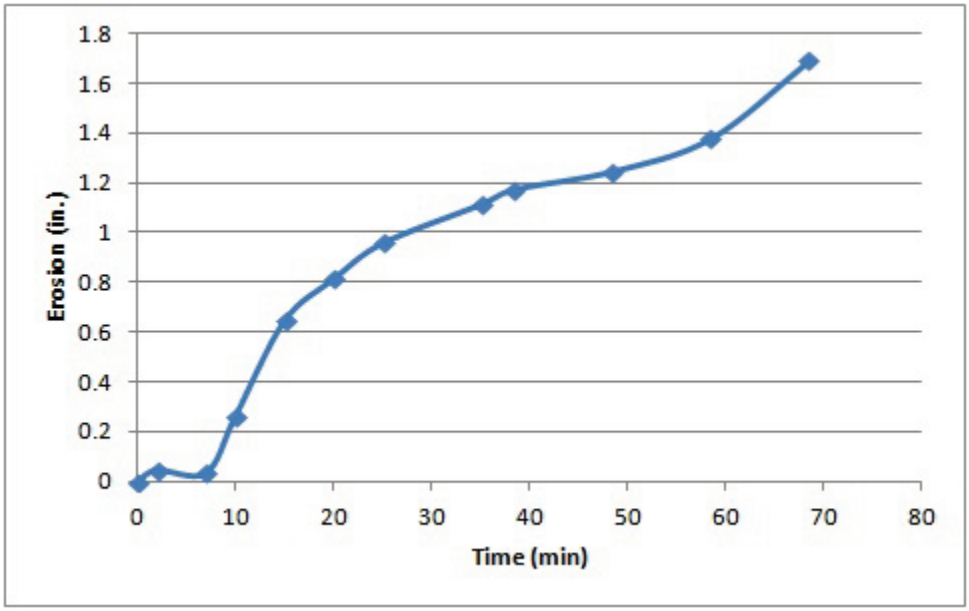

Figure A3. Test 2, (a) before and (b) after a field JET was performed.

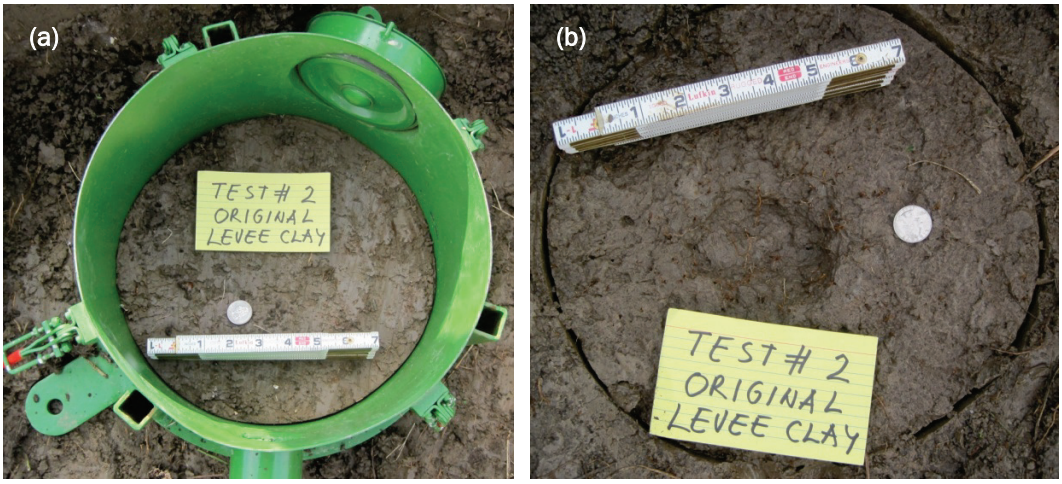

Figure A4. Test 2, cumulative erosion depth (in.) versus time (min).

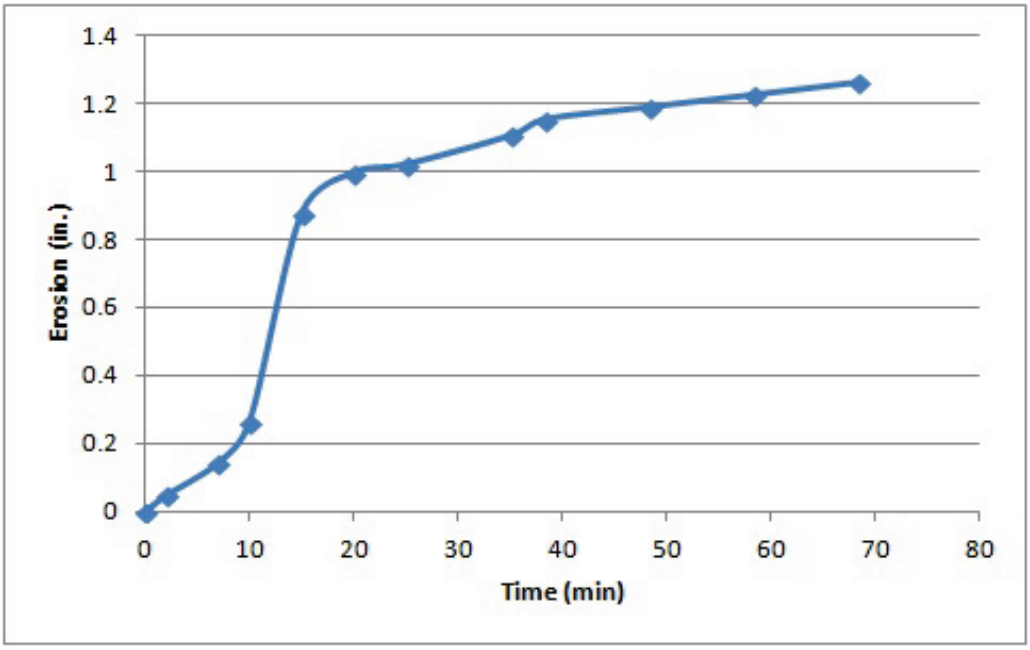

Figure A5. Test 3, (a) before and (b) after a field JET was performed.

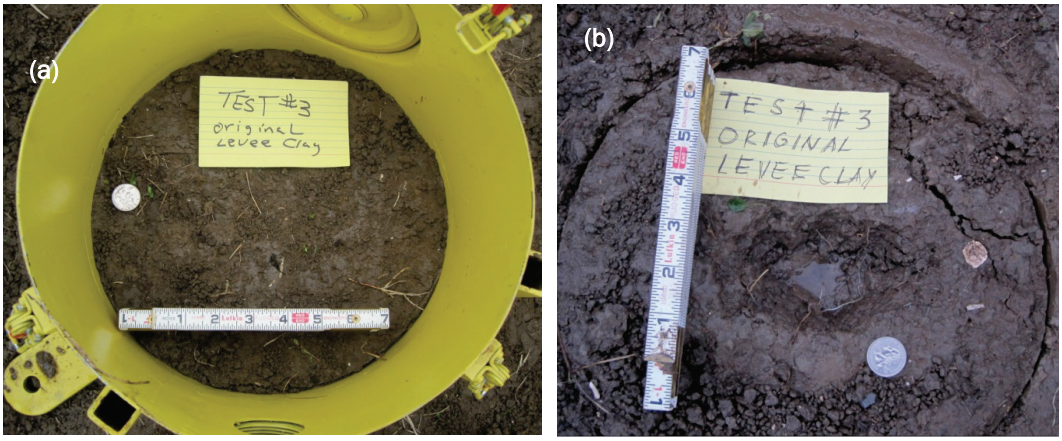

Figure A6. Test 3, cumulative erosion depth (in.) versus time (min).

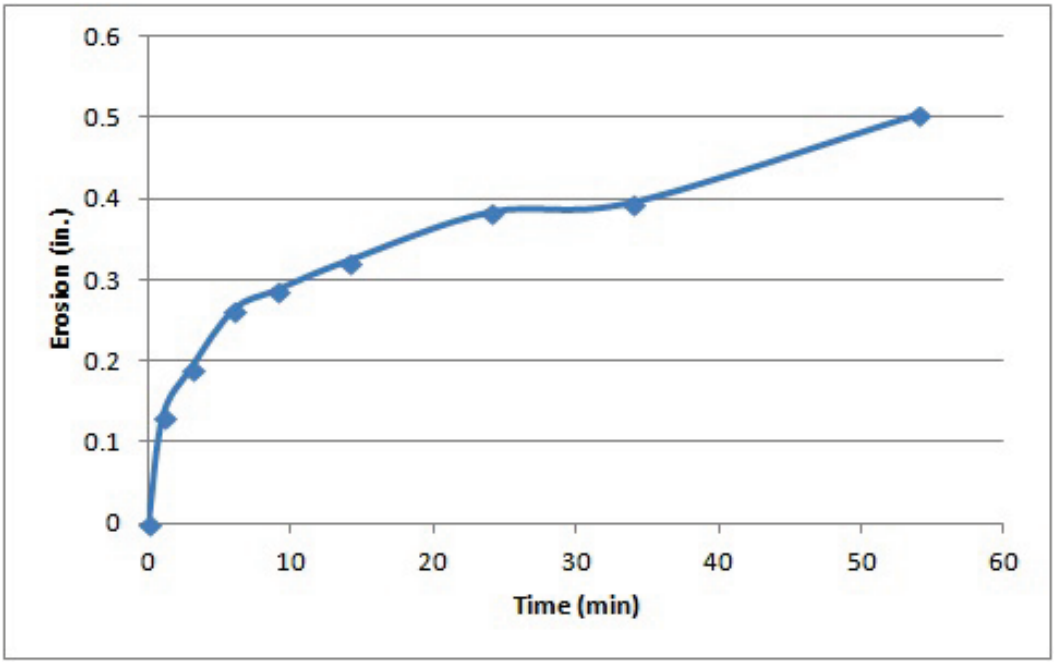

Figure A7. Test 4, (a) before and (b) after a field JET was performed.

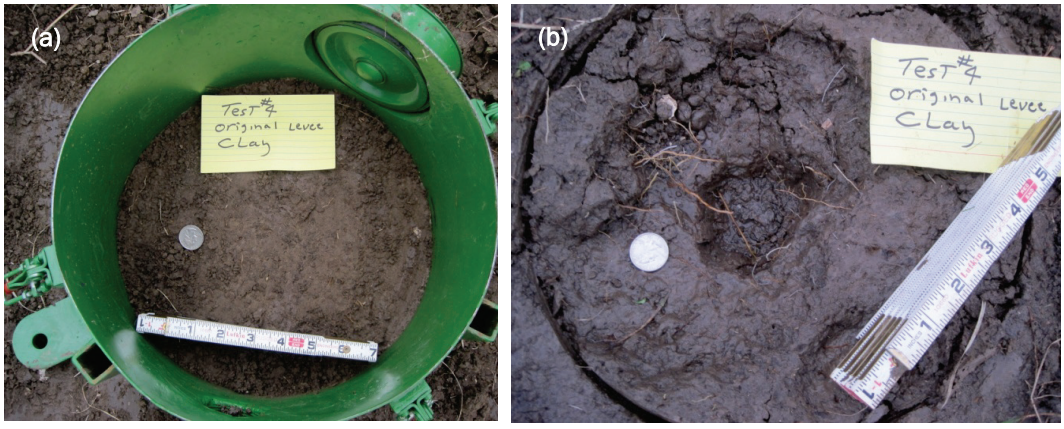

Figure A8. Test 4, cumulative erosion depth (in.) versus time (min).

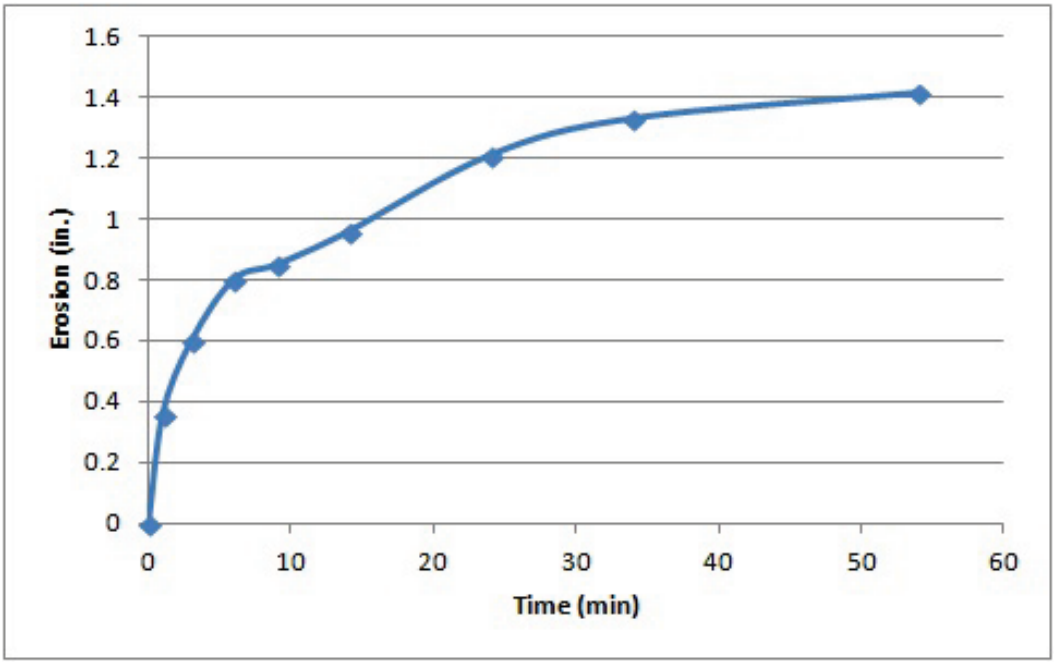

Appendix B: Levee Segment Treated with Fly-Ash/Bed-Ash

Figure B1. Test 5, (a) before and (b) after a field JET was performed.

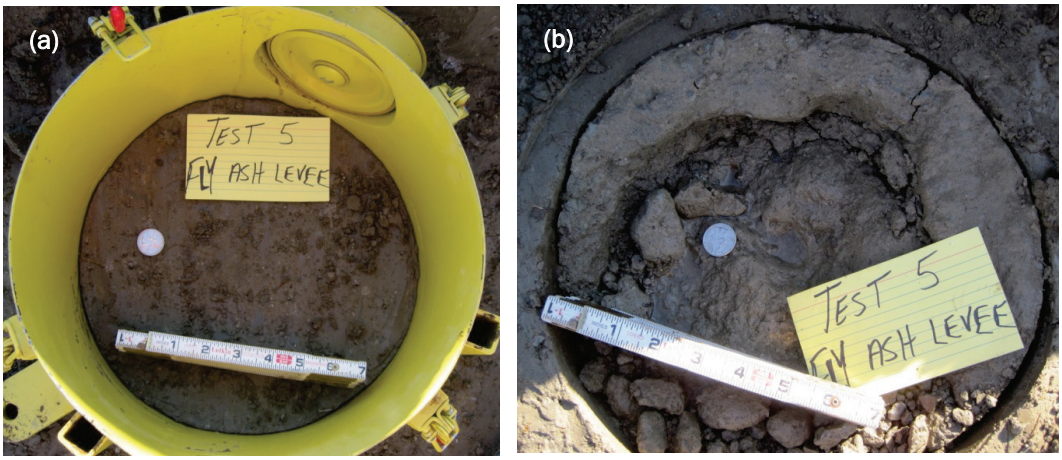

Figure B2. Test 5, cumulative erosion depth (in.) versus time (min).

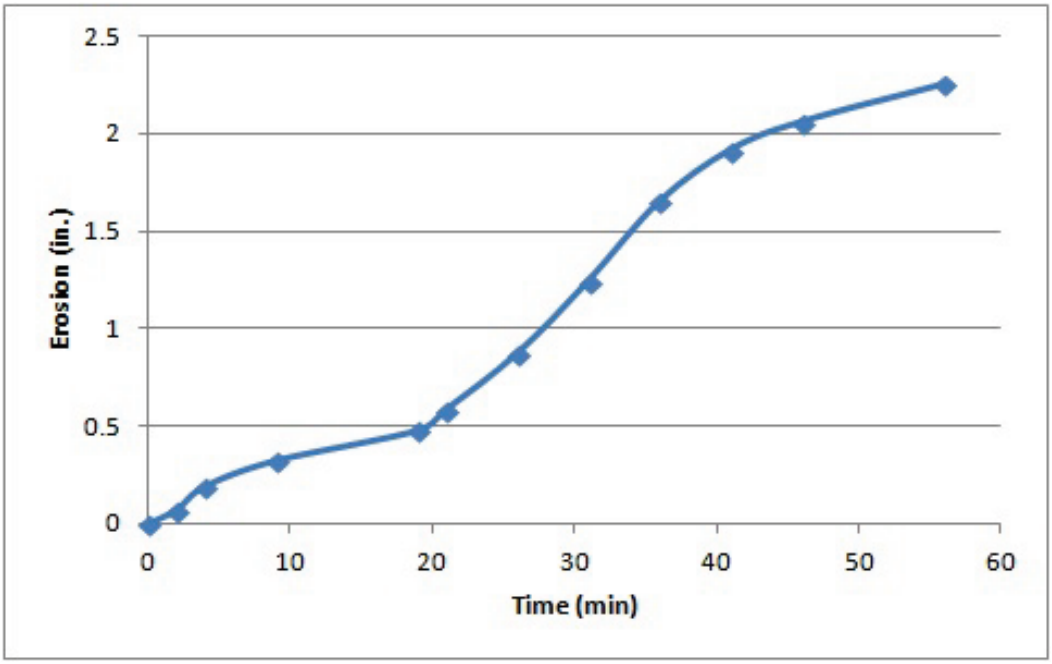

Figure B3. Test 6, (a) before and (b) after a field JET was performed.

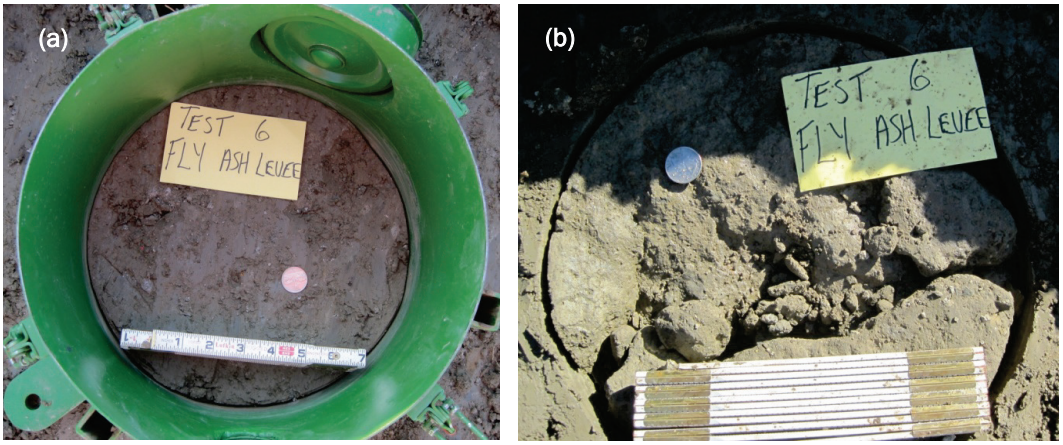

Figure B4. Test 6, cumulative erosion depth (in.) versus time (min).

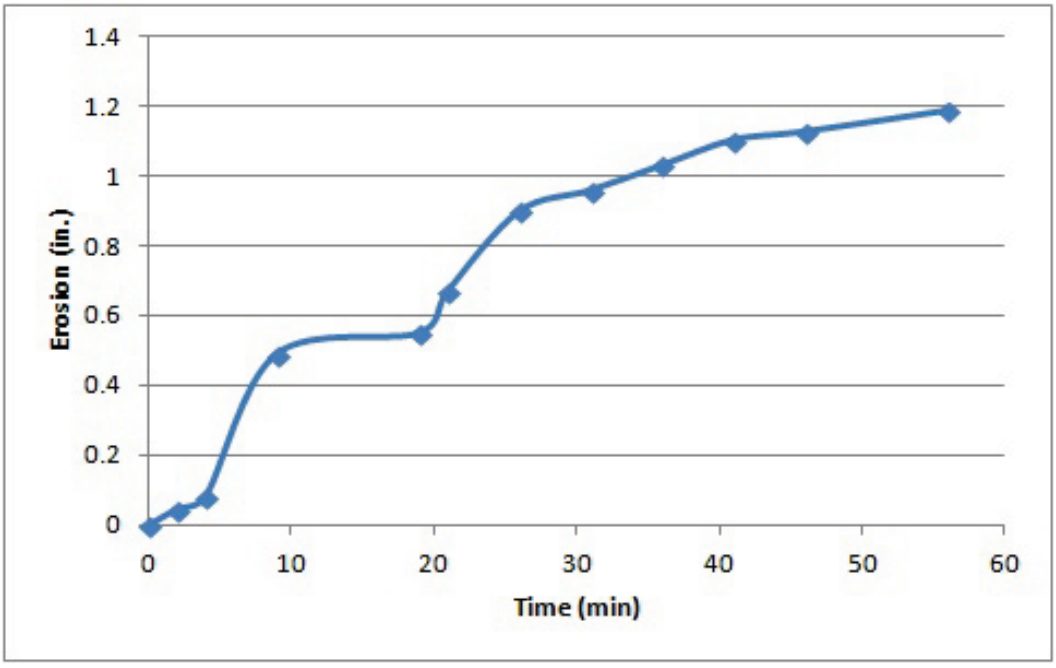

Figure B5. Test 7, (a) before and (b) after a field JET was performed.

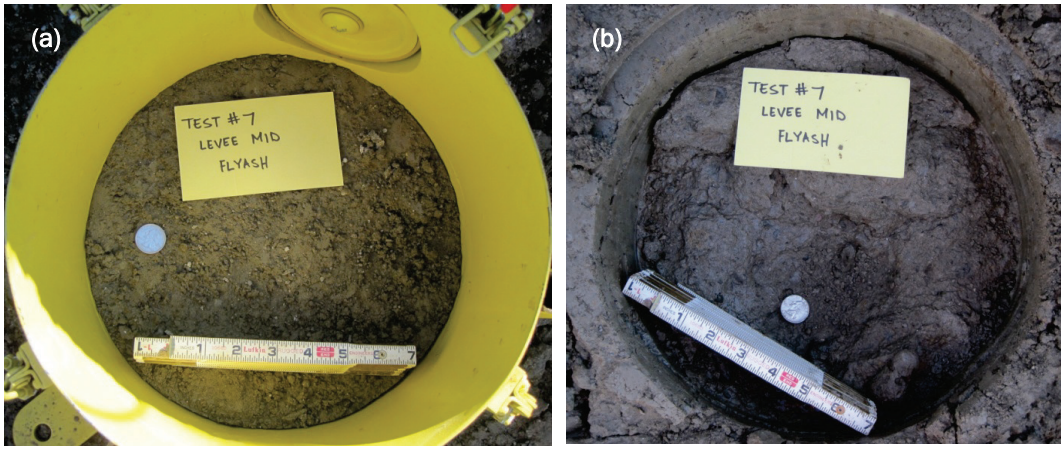

Figure B6. Test 7, cumulative erosion depth (in.) versus time (min).

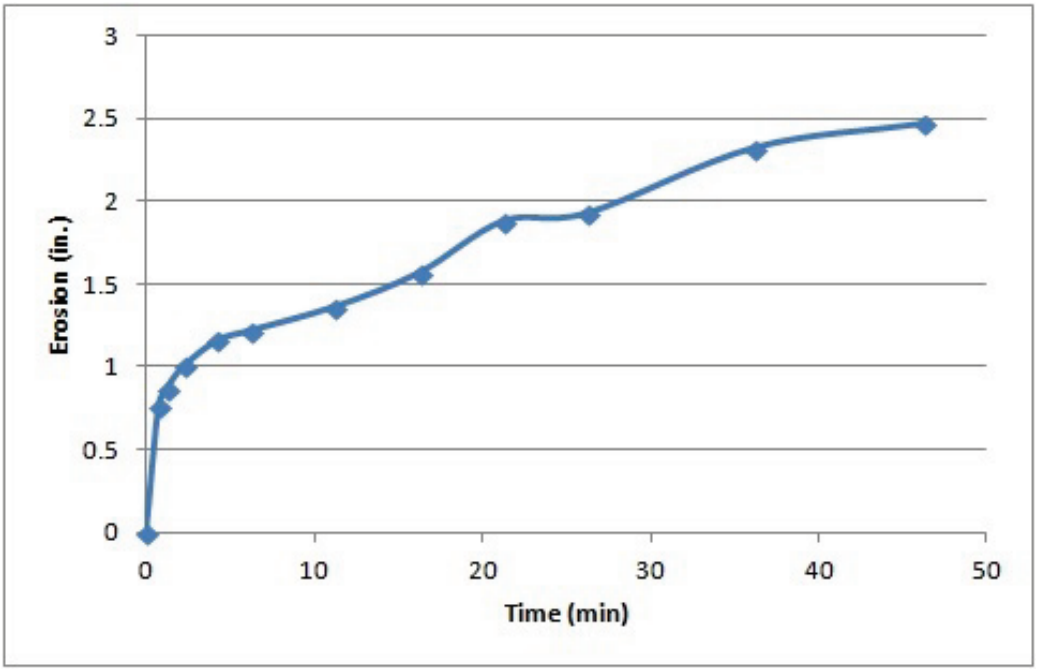

Figure B7. Test 8, (a) before and (b) after a field JET was performed.

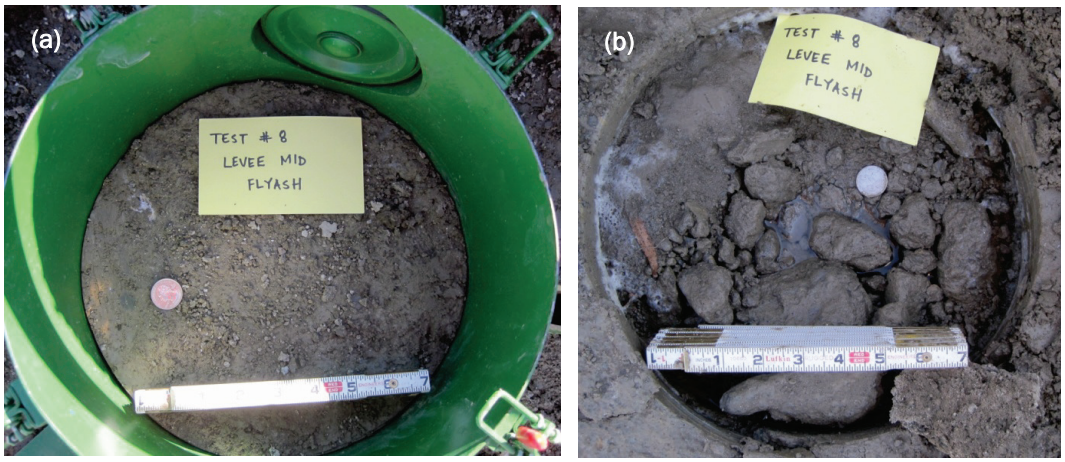

Figure B8. Test 8, cumulative erosion depth (in.) versus time (min).

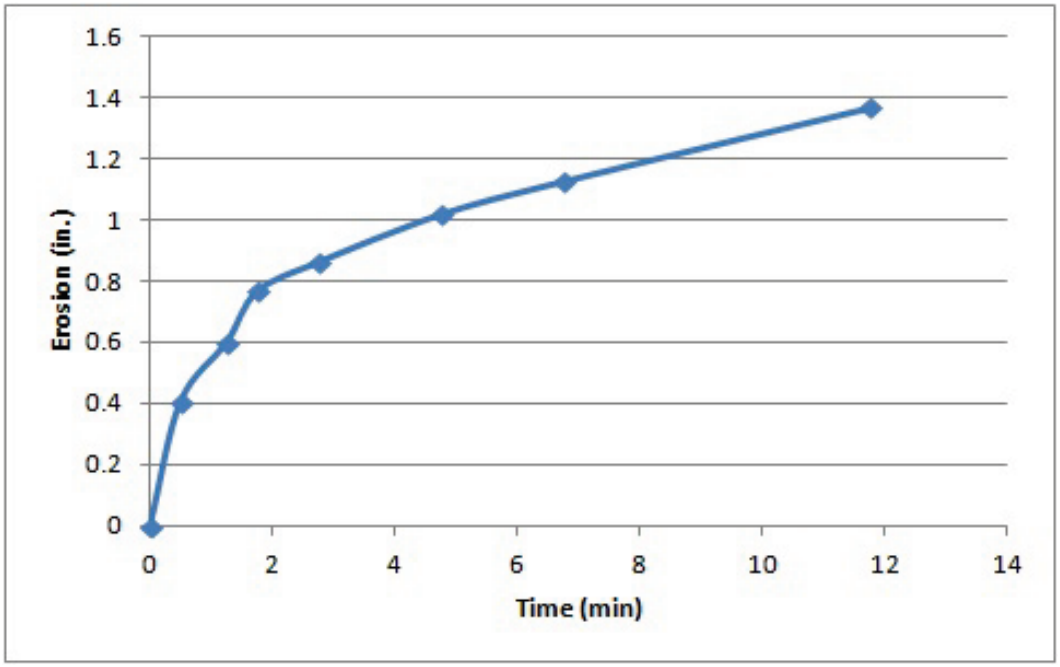

Figure B9. Test 13, (a) before and (b) after a field JET was performed.

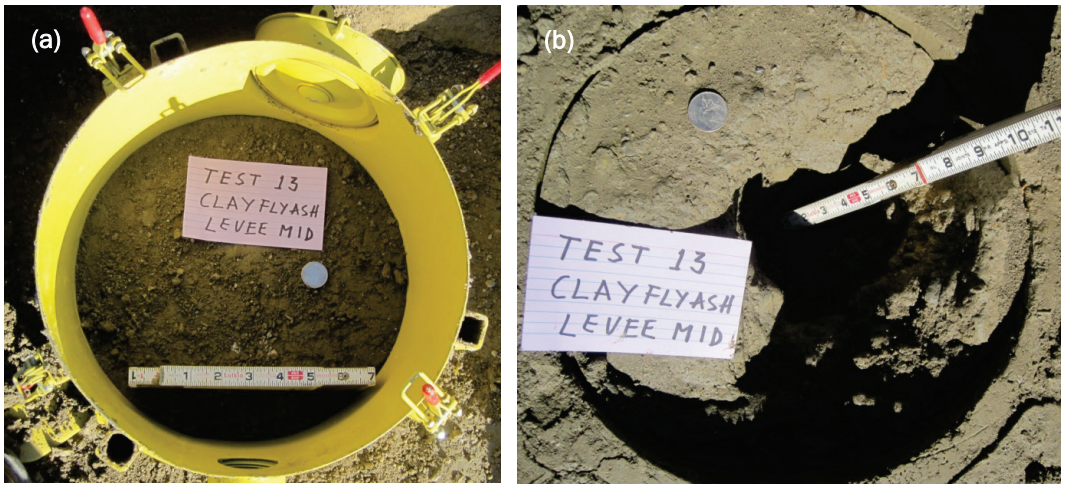

Figure B10. Test 13, cumulative erosion depth (in.) versus time (min).

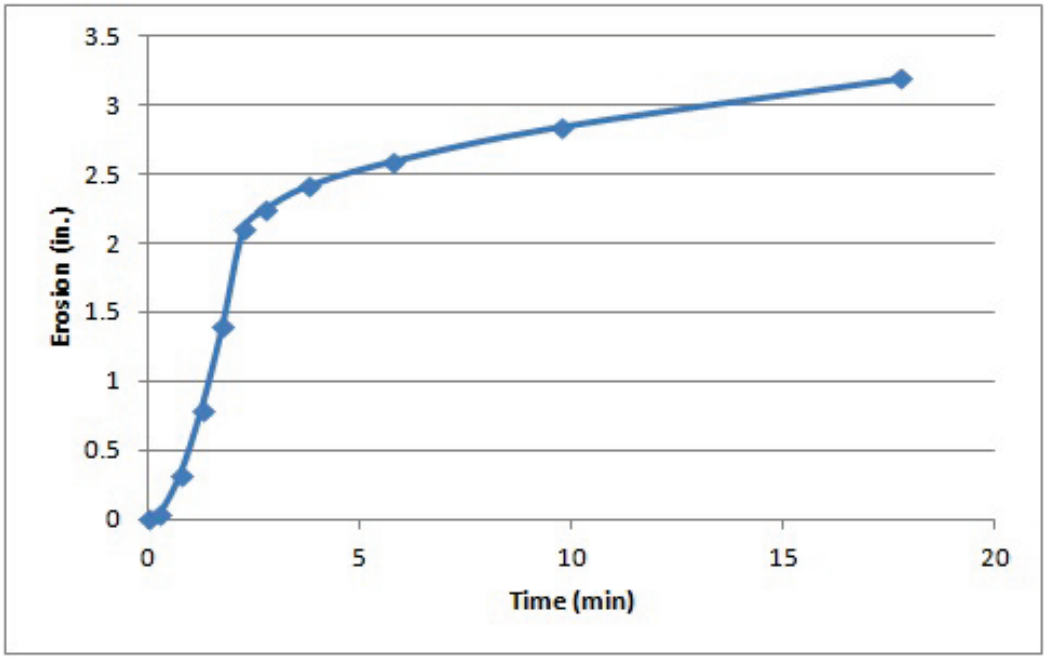

Figure B11. Test 14, (a) before and (b) after a field JET was performed.

Figure B12. Test 14, cumulative erosion depth (in.) versus time (min).

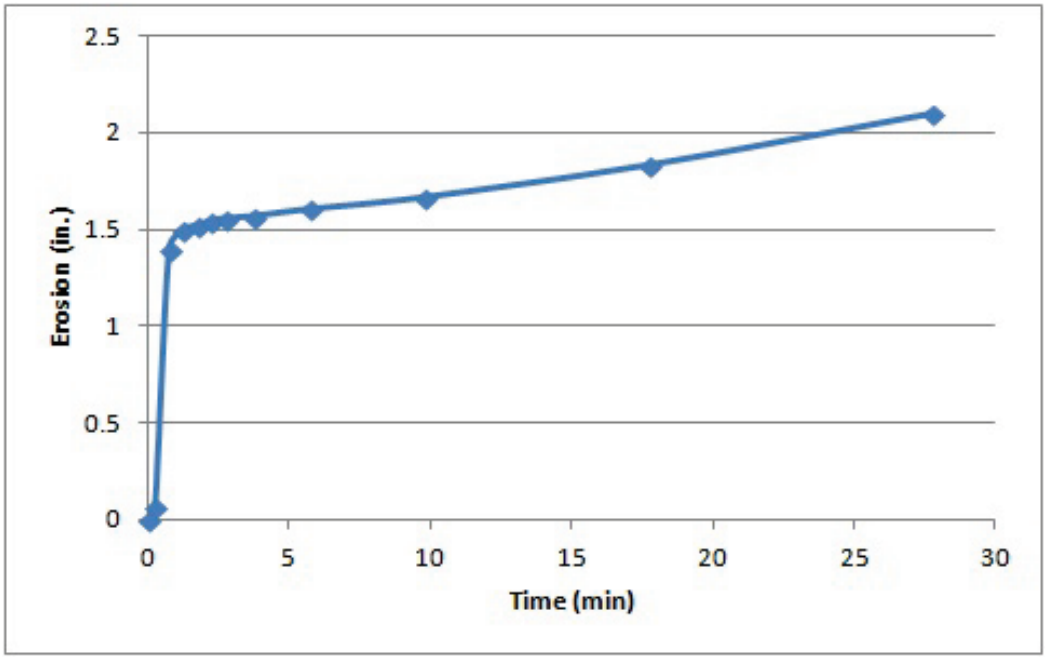

Figure B13. Test 15, (a) before and (b) after a field JET was performed.

Figure B14. Test 15, cumulative erosion depth (in.) versus time (min).

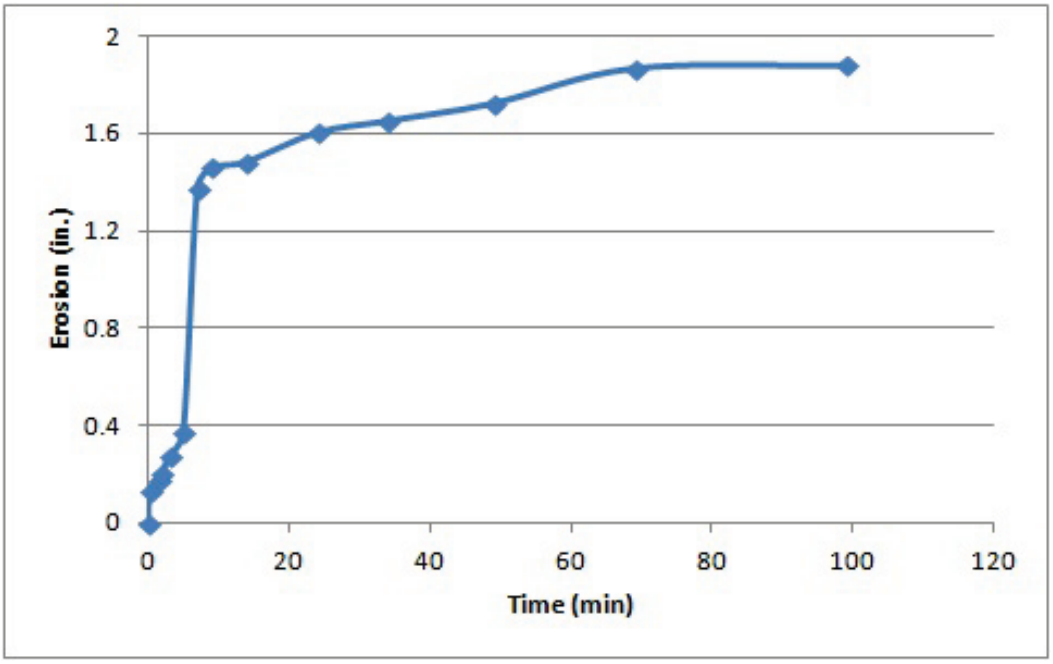

Figure B15. Test 16 (a) before and (b) after a field JET was performed.

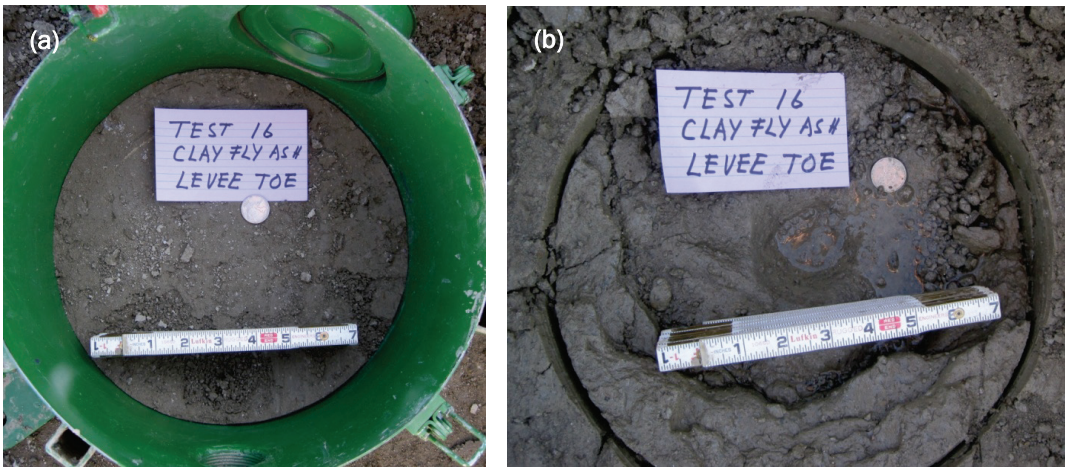

Figure B16. Test 16, cumulative erosion depth (in.) versus time (min).

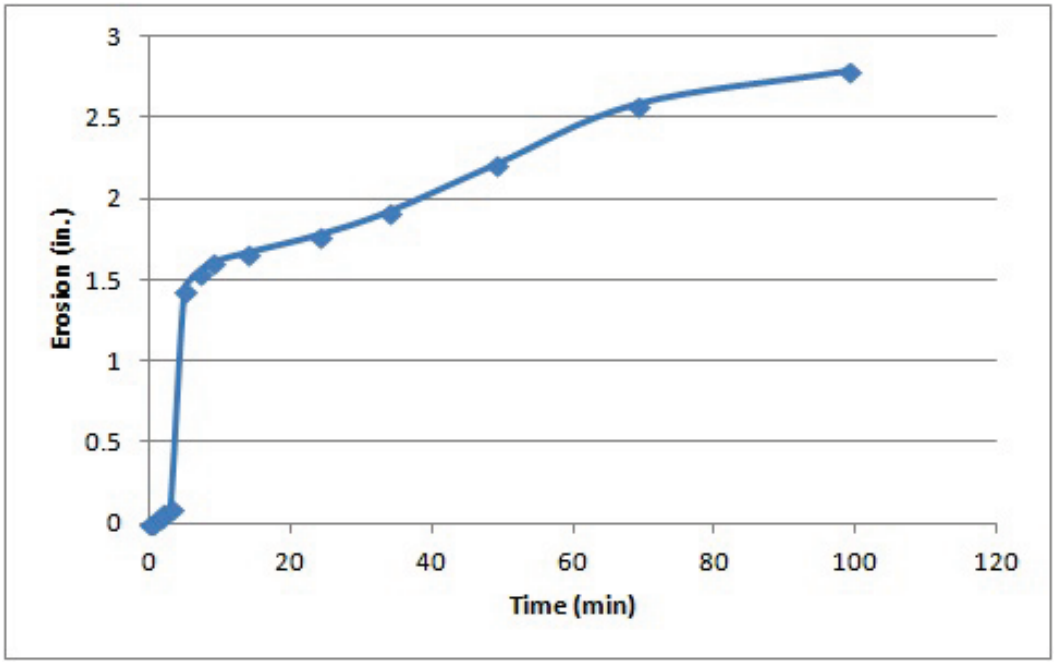

Appendix C: Levee Segment Treated with Lime

Figure C1. Test 9 (a) before and (b) after a field JET was performed.

Figure C2. Test 9, cumulative erosion depth (in.) versus time (min).

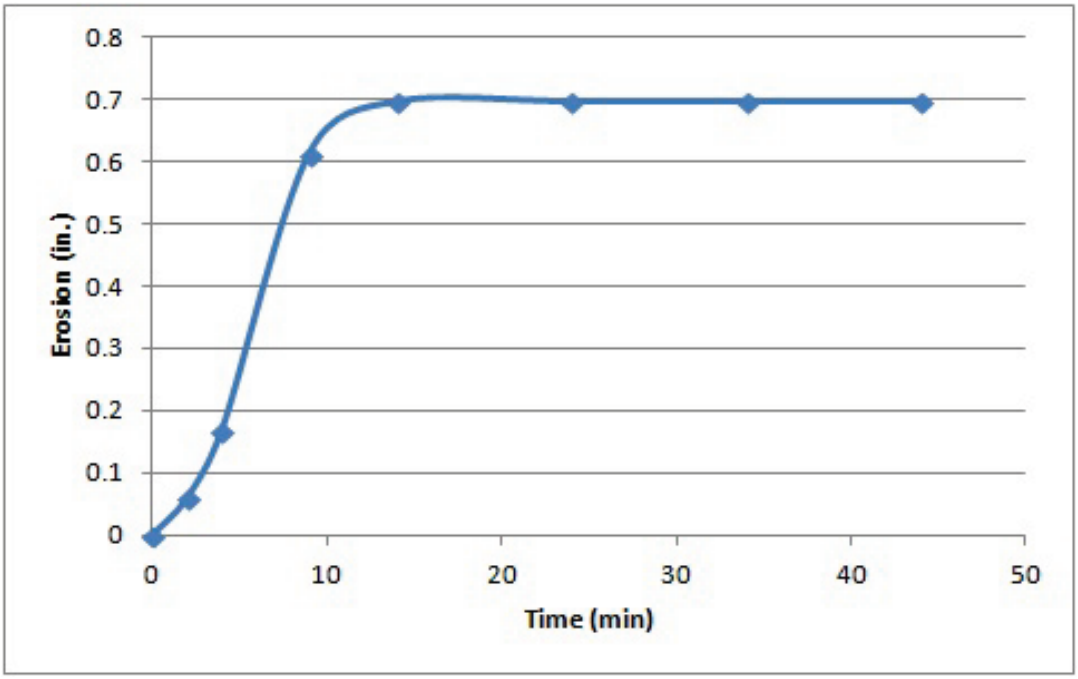

Figure C3. Test 10 (a) before and (b) after a field JET was performed.

Figure C4. Test 10, cumulative erosion depth (in.) versus time (min).

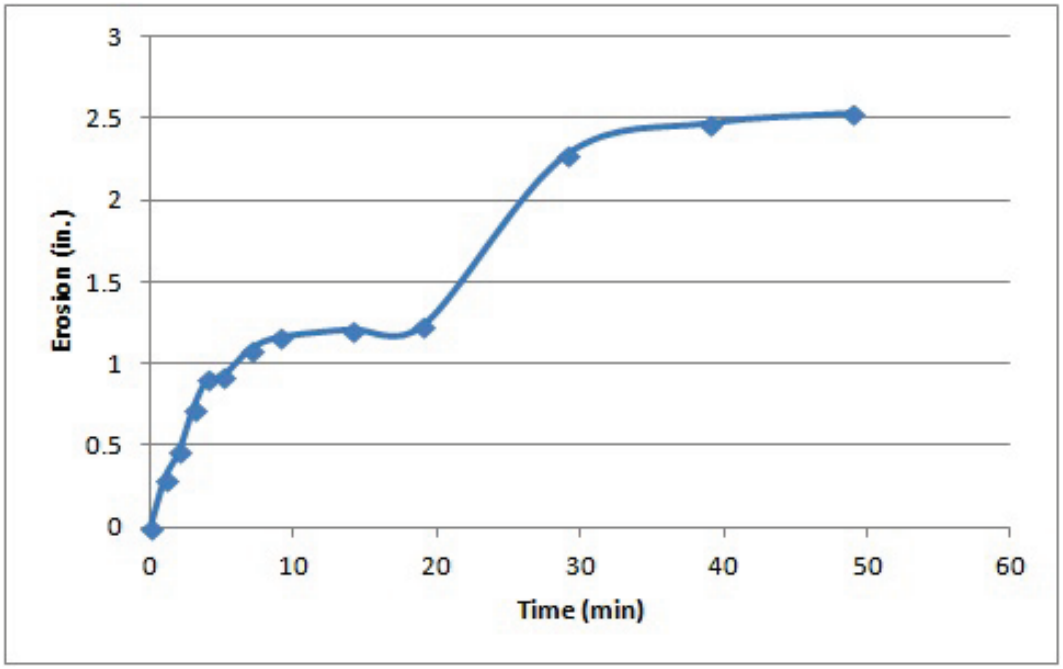

Figure C5. Test 11 (a) before and (b) after a field JET was performed.

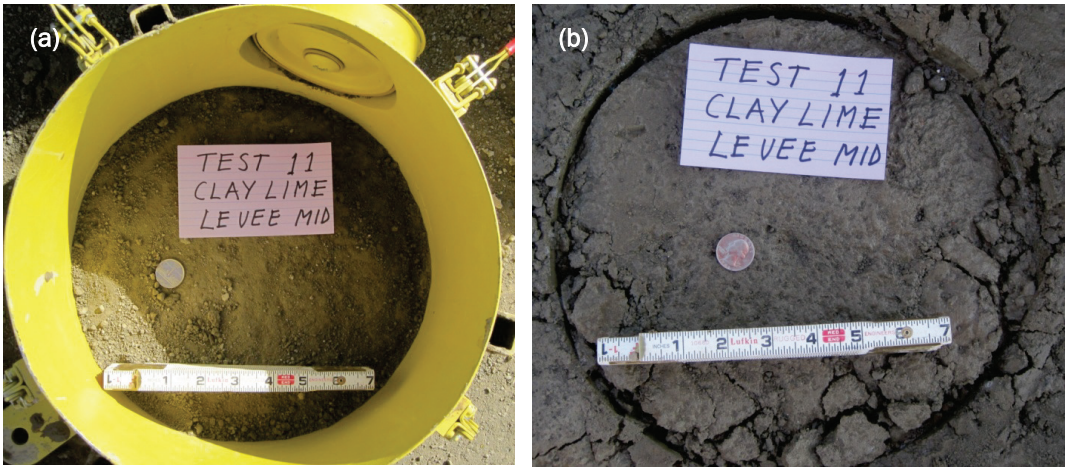

Figure C6. Test 11, cumulative erosion depth (in.) versus time (min).

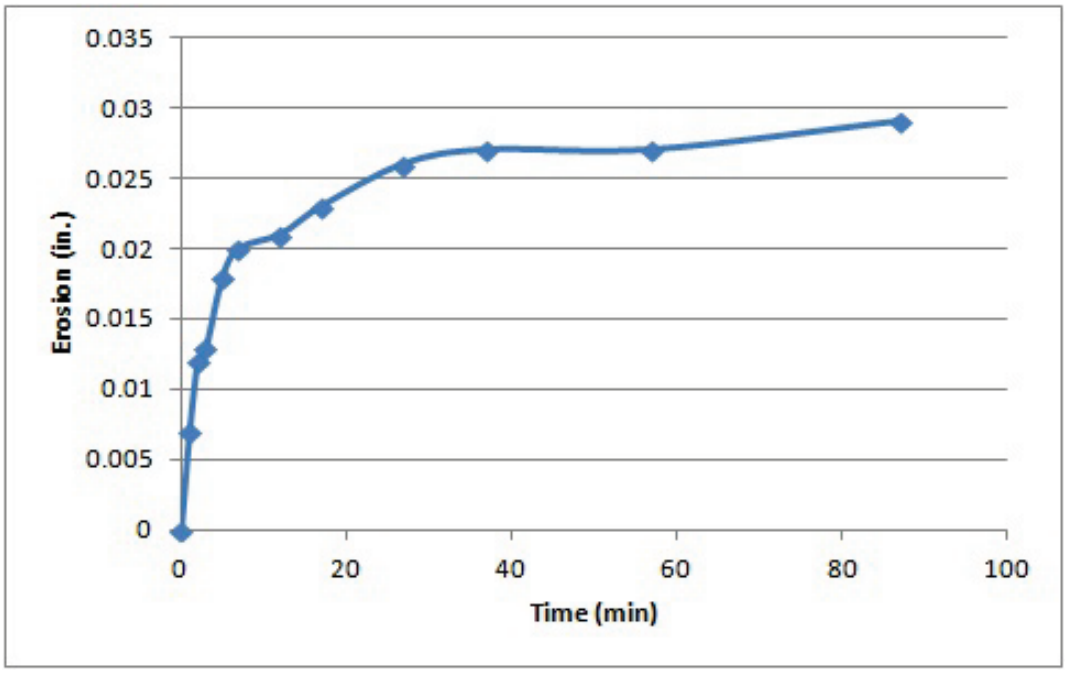

Figure C7. Test 12 (a) before and (b) after a field JET was performed.

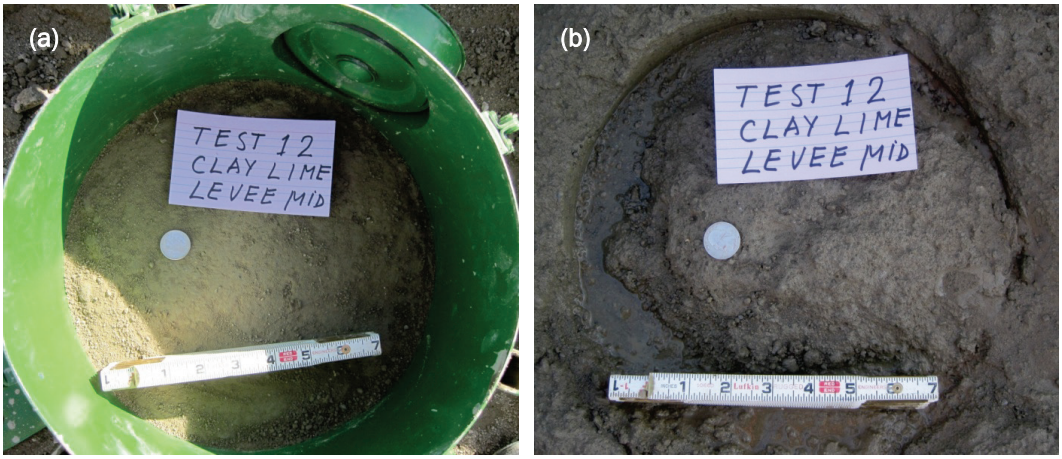

Figure C8. Test 12, cumulative erosion depth (in.) versus time (min).

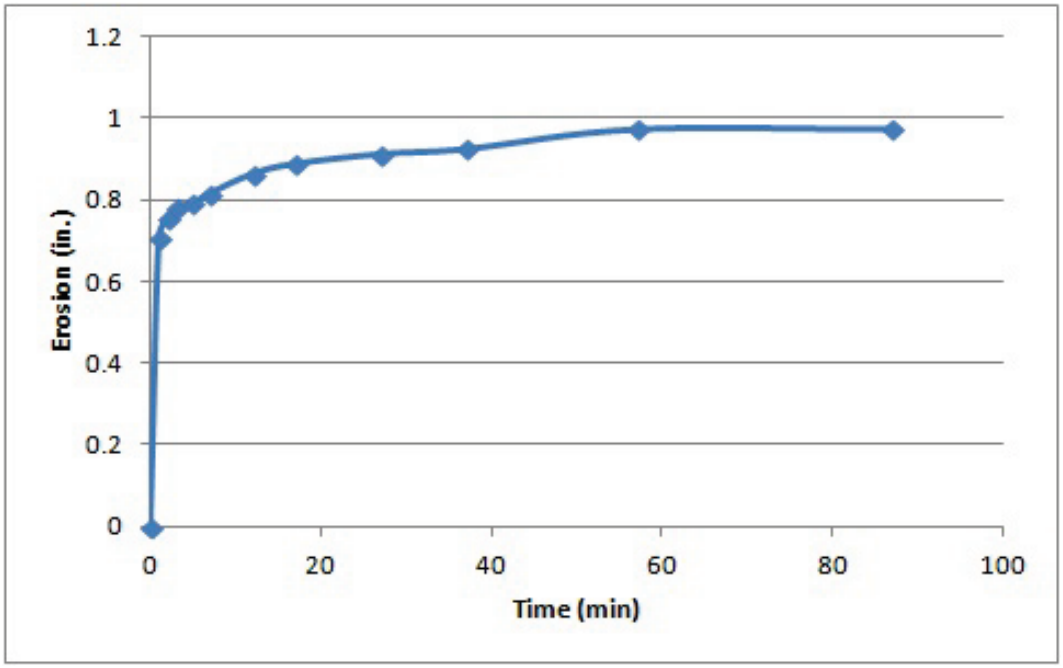

REPORT DOCUMENTATION PAGE

Form Approved
OMB No. 0704-0188

1. REPORT DATE *(DD-MM-YYYY)*	2. REPORT TYPE	3. DATES COVERED *(From - To)*
June 2015		

4. TITLE AND SUBTITLE

Field Jet Erosion Tests on the Mississippi River Collocated Demonstration Section, Plaquemines Parish, Louisiana

5a. CONTRACT NUMBER

5b. GRANT NUMBER

5c. PROGRAM ELEMENT NUMBER

6. AUTHOR(S)

Johannes L. Wibowo, Perry A. Taylor, Bryant A. Robbins, and Eric W. Smith

5d. PROJECT NUMBER

5e. TASK NUMBER

5f. WORK UNIT NUMBER

7. PERFORMING ORGANIZATION NAME(S) AND ADDRESS(ES)

Geotechnical and Structures Laboratory
U.S. Army Engineer Research and Development Center
3909 Halls Ferry Road
Vicksburg, MS 39180-6199

8. PERFORMING ORGANIZATION REPORT NUMBER

ERDC/GSL TR-15-13

9. SPONSORING / MONITORING AGENCY NAME(S) AND ADDRESS(ES)

U.S. Army Corps of Engineers
Washington, DC 20314-1000

10. SPONSOR/MONITOR'S ACRONYM(S)

HQUSACE

11. SPONSOR/MONITOR'S REPORT NUMBER(S)

12. DISTRIBUTION / AVAILABILITY STATEMENT

Approved for public release; distribution is unlimited.

13. SUPPLEMENTARY NOTES

14. ABSTRACT

Field jet erosion tests (JETs) were conducted by the U.S. Army Engineer Research and Development Center (ERDC) to assess the erodibility of two enlargement segments within the Mississippi River Levee (MRL) Collocated Demonstration Section in Plaquemines Parish, Louisiana. The first segment was constructed of Bonnet Carré clay with a fly-ash/bed-ash blend treatment, and the second segment was constructed of Bonnet Carré clay treated with lime. In addition, a section of untreated clay on the original levee was also tested. Overall, the field JET data showed that the clay treated with lime was categorized as resistant to very resistant. The fly-ash/bed-ash-treated clay was categorized as moderately resistant and resistant. When compared to the existing, untreated clay levee, both treatments reduced the erodibility of the soil. However, the field JET results showed that lime treatment performed better than the fly-ash/bed-ash treatment.

15. SUBJECT TERMS

Jet erosion test
Bonnet Carré clay
Lime treatment

16. SECURITY CLASSIFICATION OF:			17. LIMITATION OF ABSTRACT	18. NUMBER OF PAGES	19a. NAME OF RESPONSIBLE PERSON
a. REPORT	b. ABSTRACT	c. THIS PAGE			19b. TELEPHONE NUMBER *(include area code)*
Unclassified	Unclassified	Unclassified		53	